Review | Received 8 July 2026; Revised 5 August 2026; Accepted 6 August 2026; Published 24 August 2026
https://doi.org/10.55092/la20260008

DNA framework-enabled pathogen detection

Linlin Liu, Lu Song, Min Li* and Xiaolei Zuo

Renji Branch of National Center for Translational Medicine (Shanghai), Institute of Molecular Medicine, Shanghai Key Laboratory for Nucleic Acid Chemistry and Nanomedicine, Renji Hospital, School of Medicine, Shanghai Jiao Tong University, Shanghai, China

* Correspondence author; E-mail: limin2021@sjtu.edu.cn.

Highlights:

- Recent advances in DNA frameworks-based pathogen detection are introduced.
- The advantages of biosensors built on DNA frameworks are highlighted.
- Clinical and environmental applications are summarized.

Abstract: The rapid and accurate detection of pathogenic microorganisms is essential for controlling infectious diseases and protecting public health. Traditional methods, including microbial culture, immunoassays, and polymerase chain reaction (PCR), are limited by long turnaround times, cross-reactivity, and reliance on complex instrumentation. In recent decades, DNA frameworks have emerged as promising platforms for constructing high-performance biosensors, owing to their programmable configurations, nanoscale addressability, and dynamic responsiveness. This review summarizes the development of structural DNA nanotechnology and the functionalization strategies of DNA frameworks. We categorize major detection methods empowered by DNA frameworks into electrochemical, fluorescence, and point-of-care testing (POCT) approaches. Their practical applications in clinical diagnosis and environmental monitoring are summarized. Finally, we discuss emerging detection methods and the key challenges that remain to be addressed.

Keywords: DNA framework; DNA self-assembly; pathogen detection; POCT

1. Introduction

Infectious diseases, caused by pathogenic microorganisms such as bacteria, fungi, and viruses, induce tissue damage or inflammatory responses in the host [1]. According to the Global Burden of Disease Study, lower respiratory infections (LRIs) remained the leading cause of death among infectious diseases in 2023, accounting for 2.5 million deaths. Among these, *Streptococcus pneumoniae*, *Staphylococcus aureus* (*S. aureus*), and *Klebsiella pneumoniae* (*K. pneumoniae*) collectively contributed to 45.3% of LRI-related fatalities. Notably, 11 emerging pathogens (e.g., non-tuberculous mycobacteria and *Aspergillus* species) were responsible for over 500,000 LRI deaths [2]. More importantly, the recent COVID-19 pandemic caused by SARS-CoV-2 has resulted in more than 779 million confirmed cases

and over 7 million officially reported deaths since early 2020. The lessons learned from COVID-19 have underscored the critical importance of early detection and timely screening of emerging infectious diseases for interrupting transmission chains and reducing mortality, creating an urgent demand for rapid, sensitive, and portable pathogen surveillance technologies [3]. Although traditional microbial culture remains the gold standard for pathogen diagnosis, its lengthy turnaround time of 5–7 days often leads to missed therapeutic windows for patients [4–6]. Immunological methods, such as enzyme-linked immunosorbent assay (ELISA) and immunochromatography, suffer from limitations including cross-reactivity and poor antibody stability [1,7]. Conventional molecular biology techniques, such as reverse transcription–polymerase chain reaction (RT-PCR) and mass spectrometry, offer high sensitivity; however, their complex operational procedures, reliance on skilled personnel, and requirement for expensive instrumentation restrict their application in resource-limited settings [8–10]. Metagenomic sequencing, on the other hand, faces challenges such as short read lengths and sequencing biases, which compromise identification accuracy [11].

DNA frameworks, as a class of self-assembled and programmable DNA nanostructures with defined geometric shapes and nanoscale precision [12–16], possess several distinctive properties that make them particularly attractive for pathogen detection. First, the robust programmability of DNA nanotechnology enables the precise incorporation of diverse functional moieties, such as aptamers, DNAzymes, antibodies, and chemical ligands, at designated positions on DNA frameworks [17–19]. This design flexibility allows the rapid assembly of customized sensing platforms with high specificity, as different pathogenic targets can be recognized by simply incorporating their corresponding recognition elements [20]. Second, their highly programmable geometry provides precise control over the spacing, density, and orientation of recognition probes [21,22]. Unlike randomly immobilized probes on conventional surfaces, this ordered arrangement alleviates steric crowding and ensures that pathogen-specific recognition probes remain fully accessible for target binding, thereby substantially enhancing their affinity toward pathogenic nucleic acids or surface antigens [23–26]. Third, the intrinsic addressability of DNA frameworks, especially DNA origami structures that feature hundreds of programmable sites, allows the precise organization of multiple signal reporters at designated positions. By integrating with enzyme-catalyzed systems or clustered regularly interspaced short palindromic repeats (CRISPR)-based amplification, these well-organized reporters can generate greatly amplified signals upon pathogen recognition, substantially enhancing the sensitivity needed for detecting trace amounts of analytes, such as virus or bacteria in human bodies and in the environments [27–29]. Consequently, DNA framework-based biosensors exhibit superior sensitivity, specificity, and multiplexing capacity, making them powerful tools for pathogen detection [30,31]. Herein, we review recent advances in DNA framework-based biosensors for pathogen detection, discuss the programmable assembly and functionalization strategies of DNA frameworks, and introduce the detection methods empowered by these nanostructures, along with their practical applications in the rapid and sensitive detection of viruses and bacteria.

2. Construction and functionalization of DNA frameworks

Through stringent structural design, DNA molecules can self-assemble into DNA frameworks with diverse geometric configurations based on the Watson–Crick base-pairing principle [32–34]. Current DNA self-assembly technologies primarily include tile-based self-assembly [35], DNA origami self-assembly [36], single-stranded tile (SST) assembly [37], and meta-DNA assembly strategies [38]. This section focuses

on the construction of various two-dimensional (2D) and three-dimensional (3D) DNA nanostructures, as well as their subsequent engineering into functional platforms for biosensing.

2.1. Assembly of DNA frameworks

2.1.1. 2D DNA nanostructures

The development of 2D DNA nanostructures has followed two main routes: tile-based self-assembly and DNA origami technology. This section traces the evolution from early DNA junctions to complex 2D patterns and arrays.

Based on the four-arm branched junction proposed by Holliday as an intermediate in DNA homologous recombination, Seeman successfully constructed the first immobile four-arm junction with asymmetric branches in 1982 [39]. However, early four-arm junctions exhibited high flexibility, which resulted in poor structural stability of the assembled products and limiting their utility in higher-order structures. To address this issue, Seeman's group developed a novel rigid tile known as the DNA double-crossover (DX) (Figure 1a). This structure significantly enhanced rigidity and stability by arranging two double helices in parallel and introducing two crossover points [35]. In 1998, Winfree's group successfully assembled 2D grids with distinct topologies using the staggered cohesive ends of DX tiles. For the first time, they directly visualized the formation of 2D periodic arrays by atomic force microscopy (AFM), marking an important milestone in DNA self-assembly [40]. Subsequently, researchers developed various DX derivatives, including triple-crossover (TX) [41], 4 × 4 tile [42], and 6 × 4 tile [43,44] (Figure 1a). Through sequence design and complementary base pairing of their cohesive ends, these modules enabled programmable construction of 2D periodic crystals.

In 2006, Rothemund developed the DNA origami technique [36], in which a long single-stranded scaffold DNA is folded into defined shapes with the assistance of over 200 short "staple strands". Using a one-pot annealing method, the scaffold (M13mp18 bacteriophage genomic DNA) was mixed with a 10-fold excess of staple strands and annealed from 95 °C to 20 °C [45], yielding a variety of 2D nanostructures, including squares, rectangles, triangles, five-pointed stars, and smiley faces (Figure 1b). Researchers have also synthesized asymmetric 2D DNA nanostructures, such as a dolphin [46] (Figure 1c) and a map of China [47] (Figure 1d). Zhang and colleagues employed multi-armed junctions and variable-length antiparallel structural modules as building blocks within a DNA origami framework, by tuning the angles, curvatures, and lengths between arms, they constructed highly complex flower and bird patterns [48] (Figure 1e). However, the size of canonical DNA origami is limited by the length of the M13 scaffold. To overcome this limitation, researchers combined DNA origami with tile-based self-assembly to achieve micrometer-scale 2D DNA arrays [49] (Figure 1f). Similarly, Tikhomirov *et al*. used square origami units as tiles to assemble square arrays of approximately half a micrometer in size. By modifying or extending addressable staple strands on the array, they rendered images such as the Mona Lisa (Figure 1g) and a bacterium [50]. SST assembly offers another strategy to bypass the scaffold constraint. In 2012, Yin's group designed a 42-base single-stranded motif containing four internal binding domains that hybridize with neighboring tiles, generating a molecular canvas that comprises up to 310 addressable tiles and forms a 24-helix × 28-turn rectangular lattice. By selecting the single-stranded motifs corresponding to the desired pattern from the canvas, complex shapes can be self-assembled. Using this method, they constructed over 100 shapes (Figure 1h), including Chinese characters, numbers, and letters [37]. In

2020, Yan's group developed a submicrometer-scale six-helix bundle DNA origami structure as a meta-DNA analogue of single-stranded DNA. This innovative strategy, which enabled hierarchical self-assembly via programmed base-pairing interactions, broke the size limitation of conventional DNA origami and expanded the achievable length to over 5 μm, representing a significant step toward macroscopic DNA nanostructures [38].

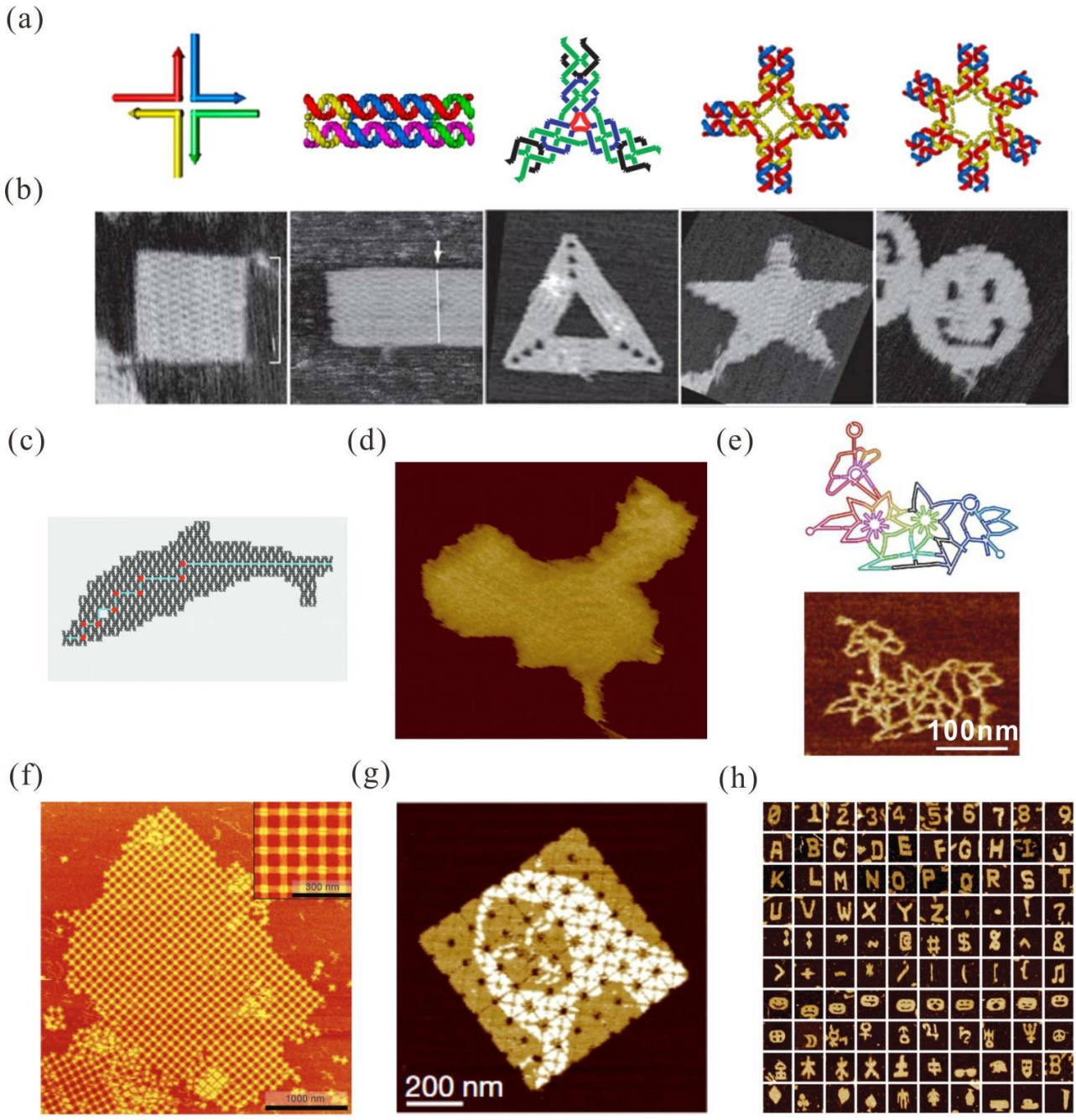

Figure 1. DNA tile-based and DNA origami-based 2D DNA nanostructures. **(a)** From left to right: 2D DNA junction. Reprinted with permission [43]. Copyright 2014 American Chemical Society. Reprinted with permission [51]. Copyright 1982 Elsevier; DX. Reprinted with permission [35]. Copyright 1996 American Chemical Society. Reprinted with permission [43]. Copyright 2014 American Chemical Society; three-point star tiles. Reprinted with permission [52]. Copyright 2008 Springer Nature; 4 × 4 tile. Reprinted with permission [43]. Copyright 2014 American Chemical

Society. Reprinted with permission [42]. Copyright 2003 American Association for the Advancement of Science; 6 × 4 tile. Reprinted with permission [43]. Copyright 2014 American Chemical Society. Reprinted with permission [44]. Copyright 2006 American Chemical Society; **(b)** From left to right: square, rectangle, triangle, star, smiling face. Reprinted with permission [36]. Copyright 2006 Springer Nature. Scale bars: 50 nm; **(c)** Asymmetrical dolphin origami. Reprinted with permission [46]. Copyright 2008 American Chemical Society; **(d)** 2D China map. Reprinted with permission [47]. Copyright 2006 Springer Nature. Scale bar: 50 nm; **(e)** Flower and bird pattern constructed with multi-arm connections. Reprinted with permission [48]. Copyright 2015 Springer Nature. Scale bar: 100 nm; **(f)** Micrometer-scale 2D DNA lattice. Reprinted with permission [49]. Copyright 2011 Wiley-VCH GmbH; **(g)** Mona Lisa. Reprinted with permission [50]. Copyright 2017 Springer Nature; **(h)** DNA canvas with different shapes. Reprinted with permission [37]. Copyright 2014 Springer Nature. Scale bar: 300 nm.

2.1.2. 3D DNA nanostructures

The extension from 2D to 3D DNA nanostructures has greatly expanded the structural diversity and application potential of DNA frameworks. This section reviews the construction of 3D DNA nanostructures, ranging from early polyhedra assembled from multi-arm junctions to complex wireframe architectures enabled by DNA origami and computational design.

In 1991, Seeman's group pioneered the construction of a covalently closed DNA cube [53] (Figure 2a, left), in which each face was formed by bending a single-stranded circular molecule and hybridizing it with complementary strands on adjacent faces. This structure represented the first 3D structure in the field of DNA nanotechnology. Subsequently, Goodman [54] and colleagues assembled a tetrahedral structure from four distinct three-segment single-stranded DNAs using a face-by-face strategy (Figure 2a, center). In 1994, Seeman's group reported a truncated octahedron (Figure 2a, right), in which four-arm junctions served as vertices and were connected via the cohesive ends of neighboring arms to form a three-dimensional framework [55]. Later, Mao's group [52,56,57] assembled a greater variety of DNA polyhedra by tuning the arm lengths, angles, and orientations of three-arm, five-arm, and six-arm junctions (Figure 2b). In order to construct 3D DNA frameworks with DNA origami technology, Shih's team developed a multilayer origami technique, in which Holliday crossovers were introduced between adjacent DNA helices to enable parallel stacking, yielding 3D nanostructures with honeycomb lattice cross-sections [58]. Through site-directed base insertions and deletions, they further constructed 3D twisted structures with precise curvatures, such as a beach ball and square-toothed gears [59] (Figure 2c). To break the constraints of lattice-based assembly and achieve more precise curvature control, Yan's group [60] assembled single-layered 3D DNA nanostructures by connecting multiple concentric rings with crossovers at defined dihedral angles, producing spherical shells, ellipsoidal shells, and flasks (Figure 2d).

Computer-assisted design algorithms have greatly facilitated the construction of complex 3D DNA origami structures. For example, Högberg's group combined origami technology with computer-aided modeling to construct various complex curved structures, including stick figures and a Stanford bunny [61] (Figure 2e). Bathe's group developed a fully automatic top-down design algorithm that generates DNA origami sequences directly from arbitrary target geometries, enabling the construction of complex wireframe polyhedra including non-spherical topologies [14] (Figure 2f). To construct larger structures, Yin *et al*. employed tripod-shaped origami monomers with tunable interarm angles as tiles, assembling

them via inter-arm connections into various polyhedral [62] (Figure 2g). Furthermore, they extended single-stranded modules from 2D tiles to 3D bricks and constructed kilodalton-scale 3D models of a teddy bear and a rabbit [63] (Figure 2h). As more DNA nanostructures were successfully assembled, researchers increasingly focused on their functional capabilities. To better exploit these structures for functional applications, Fan's group introduced the concept of framework nucleic acids in 2018 [12], systematically defining this new class of DNA structures that organize functional molecules with nanoscale precision and exhibit properties distinct from single-stranded DNA or RNA.

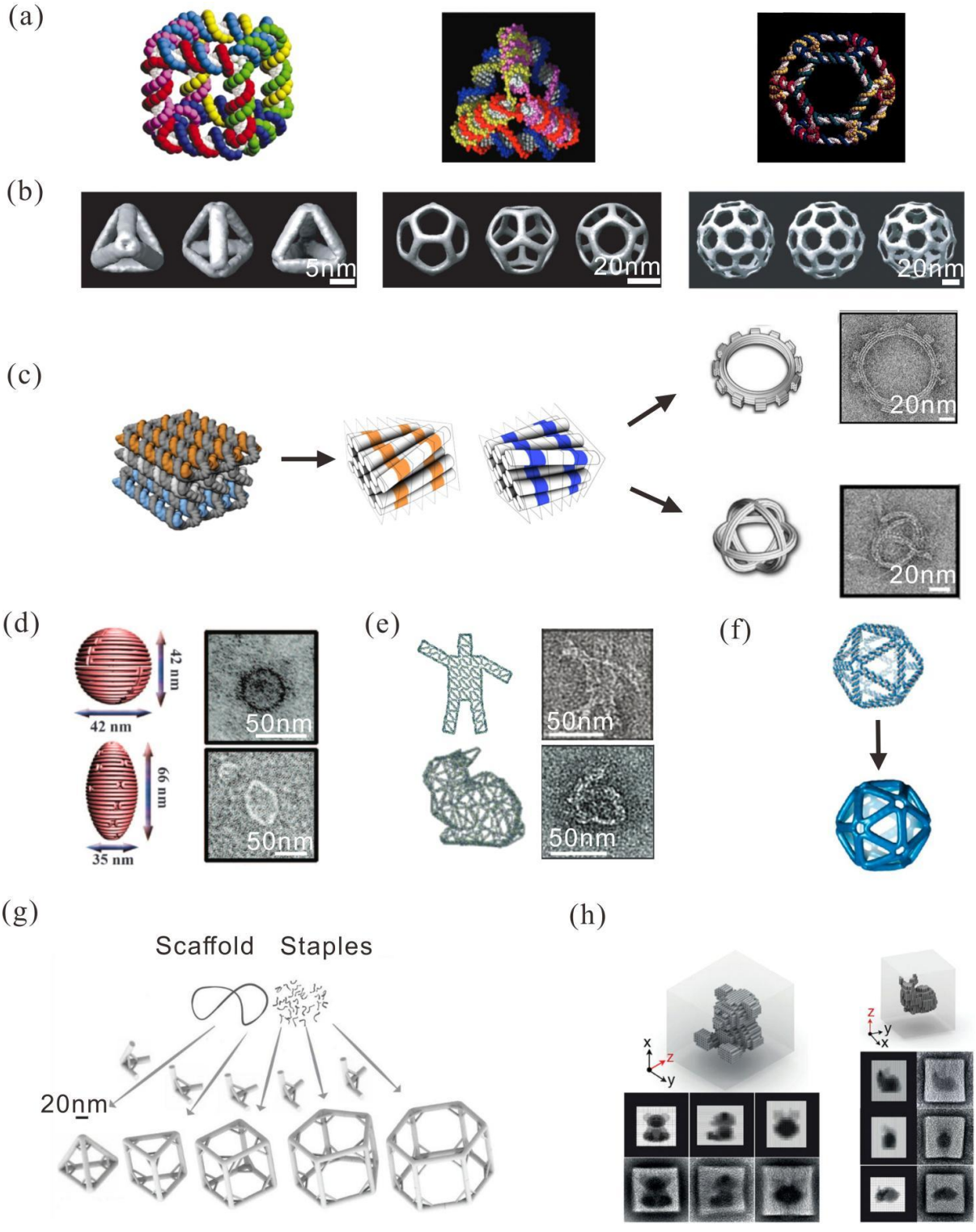

Figure 2. 3D DNA nanostructure. **(a)** From left to right: DNA cube. Reprinted with permission [64]. Copyright 2003 Springer Nature; DNA tetrahedron. Reprinted with permission [54]. Copyright 2005 American Association for the Advancement of Science; DNA octahedron. Reprinted with permission [55]. Copyright 1994 American Chemical Society; **(b)** Three views of DNA tetrahedron structure, DNA dodecahedron 3D structure and DNA buckyball structure. Reprinted with permission [52]. Copyright 2008 Springer Nature. Scale bars are 5 nm, 20 nm, and 20 nm, respectively; **(c)** The top: hierarchical assembly of monomers yields 12-tooth gears; the bottom: a sandbox constructed by base pair insertion and deletion in a honeycomb lattice. Reprinted with permission [59]. Copyright 2009 American Association for the Advancement of Science. Scale bars: 20 nm; **(d)** Spherical shells and ellipsoidal shells. Reprinted with permission [60]. Copyright 2011 American Association for the Advancement of Science. Scale bars: 50 nm; **(e)** Stick figures and a Stanford bunny. Reprinted with permission [61]. Copyright 2015 Springer Nature. Scale bars: 50 nm; **(f)** DNA wireframe icosahedron. Reprinted with permission [14]. Copyright 2016 American Association for the Advancement of Science; **(g)** Polyhedra self-assembled from DNA tripods. Reprinted with permission [62]. Copyright 2014 American Association for the Advancement of Science; **(h)** 3D teddy bear and rabbit synthesized via single-chain self-assembly strategy. Reprinted with permission [63]. Copyright 2017 Springer Nature. Scale bars: 50 nm.

2.2. Functionalization of DNA frameworks

DNA frameworks can be endowed with sensing capabilities through functionalization with two types of elements: recognition probes responsible for specific target capture, and signal probes responsible for signal transduction [65–67]. The synergistic integration of these two types of elements enables DNA frameworks to function as versatile sensing platforms.

2.2.1. Recognition probes

Conventional pathogen identification strategies typically immobilize nucleic acid-based probes or antibodies onto the surface of the particles and chips. However, these methods suffer from random probe orientation, significant steric hindrance, and uncontrollable surface density, resulting in low binding affinity. In contrast, DNA frameworks, as 2D or 3D nanostructures with nanoscale precision, can precisely modulate the spatial location, orientation and valency of the recognition probe at the nanoscale through base complementary pairing or chemical coupling. This capability significantly improves the recognition affinity and specificity. Currently, the recognition elements employed in the functionalization of DNA frameworks fall into two main categories: nucleic acid-based probes and protein-based probes.

Nucleic acid probes are DNA or RNA-based recognition elements that can be categorized into single-stranded probes, structure-responsive probes (such as molecular beacons), and functional nucleic acids (such as aptamers and DNAzymes). These probes can be directly synthesized at the specific position of a DNA framework through covalent extension of the scaffold sequence. Alternatively, based on Watson–Crick base pairing, a “handle” sequence (15–20 nucleotides) can be extended from the framework vertex, allowing the recognition probe to be non-covalently loaded via hybridization [68,69].

In the following section, we will discuss the construction of DNA framework-based probes according to their target types: nucleic acid targets and non-nucleic acid targets.

For nucleic acid detection, Guo *et al*. designed a tetrahedral DNA framework (TDF) carrying a 10-nt single-stranded overhang as the recognition domain for miRNA-21 [70] (Figure 3a). To achieve multiplexed detection, Qiu *et al*. attached four distinct X-shaped probes to the four vertices of a TDF, achieving simultaneous genotyping of all four possible base variations at a single site to identify clarithromycin resistance-associated single-nucleotide variants in Helicobacter pylori [71]. Without relying on base pairing with target sequences, aptamers spontaneously fold into high-affinity 3D structures to specifically detect non-nucleic acid targets [72–75], such as proteins, small molecules, and ions [76,77]. When displayed on DNA frameworks, aptamers can achieve enhanced binding through multivalent effects. For instance, Ahmadi *et al*. conjugated ten copies of *S. aureus* protein A-binding aptamers to the edges of a DNA origami nanostructure, achieving superior bacterial recognition with approximately 4.7-fold higher affinity compared to the free aptamer [78] (Figure 3b). To achieve simultaneous detection of multiple types of targets, Tu *et al*. confined a DNAzyme inside a DNA nanocage by hybridizing two linker sequences on the DNAzyme with complementary strands attached to opposite edges of the nanocage [79]. This design allowed the DNA framework-hosted DNAzyme to serve as a dual-recognition probe for both miR-21 and Zn^{2+}. Collectively, nucleic acid probes exhibit good stability, target diversity, and ease of chemical synthesis, making these functionalized DNA frameworks ideal platforms for biosensing [30,80–82].

Beyond nucleic acid probes, protein-based recognition probes, primarily antibodies, have also been integrated into DNA frameworks. Antibodies are widely employed for target capture due to their high affinity and specificity [83]. To attach antibodies to DNA frameworks, various strategies have been developed. For instance, Zhang and coworkers anchored digoxin molecules at varying distances on a triangular DNA origami as artificial epitopes [84]. Based on the principle of antigen-antibody specific recognition, anti-digoxin IgGs captured digoxin molecules in monovalent or bivalent forms via their Fab domains, thereby connecting to the origami. This study revealed that the optimal distance for bivalent binding of IgG is approximately 10 nm (Figure 3c). To enhance the versatility of antibody-DNA framework assembly beyond specific antigen-antibody pairs, Pradhan *et al*. functionalized a 3D wireframe DNA origami with anti-GFP nanobodies via DNA hybridization [85]. The nanobody was fused with a SNAP-tag, which covalently combines with a benzylguanine-modified oligonucleotide. Hybridization of this conjugate with complementary handles evenly distributed on the origami surface enabled multivalent presentation of nanobodies, achieving up to 60 copies per scaffold (Figure 3d). However, this strategy relies on genetic fusion and is not directly applicable to full-sized IgGs. To overcome this limitation and extend DNA framework functionality to conventional antibodies, Rosier *et al*. [86] conjugated antibodies to oligonucleotides using a photocrosslinkable protein G adapter that binds to the Fc region, subsequently, the conjugates were hybridized to complementary handles on DNA origami surfaces. In contrast to Rosier's design, which requires pre-conjugation of antibodies with oligonucleotides, Ouyang *et al*. achieved direct, orientation-controlled immobilization of unmodified antibodies within DNA origami cavities through a synergistic combination of tris(nitrilotriacetic acid)-Ni^{2+} coordination and NHS ester crosslinking [87] (Figure 3e). Despite the superior affinity of antibodies, their high production cost and potential for cross-reactivity have prompted researchers to seek alternative biospecific recognition elements [88–90].

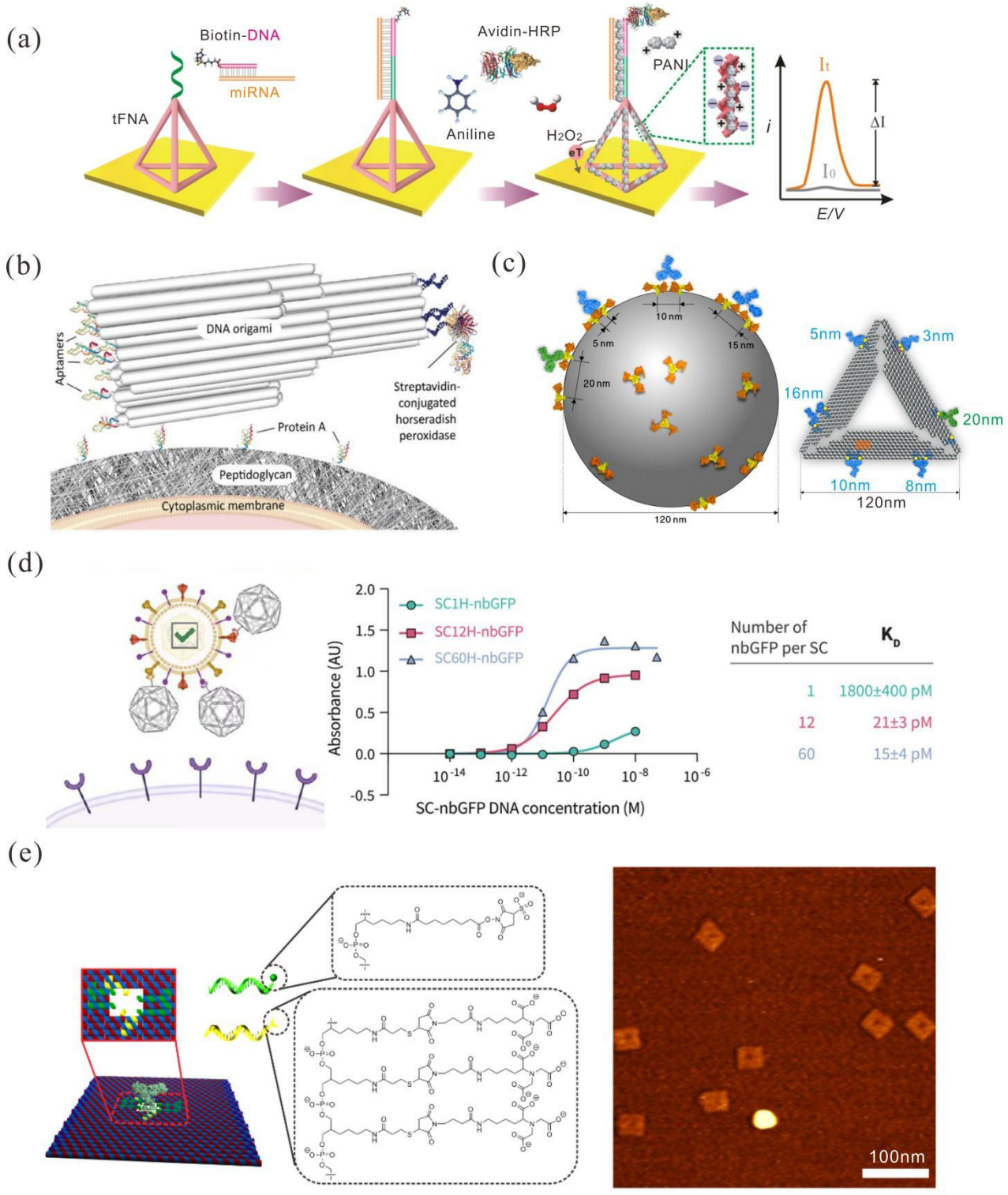

Figure 3. Immobilization of Recognition Probes on DNA Frameworks. **(a)** A TDF-mediated electrochemical sensor for miRNA-21 detection. Reprinted with permission [70]. Copyright 2022 American Chemical Society; **(b)** Staphylococcus aureus biosensor based on DNA origami. Reprinted with permission [78]. Copyright 2024 Elsevier; **(c)** Triangular DNA origami-based virus epitope mimetics for IgG Binding. Reprinted with permission [84]. Copyright 2020 Springer Nature; **(d)** Pseudorabies virus transmission blocked by spherical nucleic acid. Reprinted with permission [85]. Copyright 2023 American Chemical Society; **(e)** Spatially controlled antibody anchoring in DNA origami cavities. Reprinted with permission [87]. Copyright 2017 Wiley-VCH GmbH.

2.2.2. Signal probes

Beyond target recognition, the functionalization of DNA frameworks with various signaling molecules and nanomaterials is essential for translating binding events into measurable signals. DNA frameworks provide precise spatial control over the loading position, stoichiometric ratio, and distance from the recognition interface, which is critical for the design of sensitive and reliable signal reporting systems [91–94].

To achieve the combination of DNA framework with fluorescent signal molecules, early strategies mainly relied on non-covalent insertion of dyes into double-stranded DNA regions. For instance, Qiao's group embedded SYBR Green I specifically into the base pairs of double-stranded DNA within a DNA nanotriangle framework for fluorescence signal output [20]. However, such intercalation-based approaches suffer from poor spatial control and nonspecific signal output due to the lack of sequence specificity. To overcome these limitations, covalent chemical modification strategies have been developed, enabling precise and programmable signal output. Zhou *et al*. co-labeled a fluorophore (FAM) and a quencher (BHQ) at the same vertex of a TDF to construct an "off-on" fluorescent sensor for the detection of DNA methyltransferase [95]. Taking a different approach, Brannetti *et al*. covalently conjugated fluorophores (Cy3, Cy5, or FAM) to the termini of specific DNA strands. These fluorophore-labeled strands were self-assembled with unlabeled strands into DNA tiles, which further polymerized into micron-scale fluorescent structures. These scaffolds served as signal reporters in lateral flow assays, enabling sensitive and multiplexed detection of antibodies, proteins, and small molecules [96] (Figure 4a). To achieve precise regulation of signal molecule interactions, Grzedowski *et al*. employed a DNA nanocube that precisely controlled the distance and relative orientation of Alexa Fluor 488 and Alexa Fluor 647, consequently modulating fluorescence resonance energy transfer (FRET) efficiency and enabling target detection [97].

To further enhance detection sensitivity, DNA frameworks have also been employed as programmable scaffolds for controlled signal amplification. Nucleic acid reaction-based signal amplification strategies have been integrated to further increase signal output. Zhang and coworkers attached two hairpins (H1 and H2) to the sticky ends of a tetrahedral framework. H1, labeled with Cy5 and BHQ, served as the target recognition probe. When the target triggered the hybridization chain reaction (HCR), an amplified fluorescence signal was generated for high-sensitivity imaging [98] (Figure 4b). Enzyme-mediated signal amplification has also been explored on DNA frameworks. Zhao *et al*. used a TDF to multivalently anchor alkaline phosphatase (ALP)-labeled streptavidin; prostate-specific antigen (PSA)-triggered TDF-ALP release enabled ALP-mediated colorimetric PSA detection [99]. This TDF-ALP platform achieved a limit of detection (LOD) of 36 pg/mL, which improved 24-fold in sensitivity over a ssDNA-based control without multivalent ALP loading (Figure 4c). In contrast to this colorimetric readout, Zhu *et al*. achieved a fluorescence-based signal amplification by encoding multicomponent nucleic acid enzymes (MNAzymes) directly into TDFs [100]. Following target miRNA recognition, the MNAzyme formed an active DNAzyme structure that cleaved fluorescent substrates while releasing the intact target for subsequent cleavage cycles. This circular amplification strategy enabled sensitive multiplexed imaging of miR-21 and miR-155 in living cells.

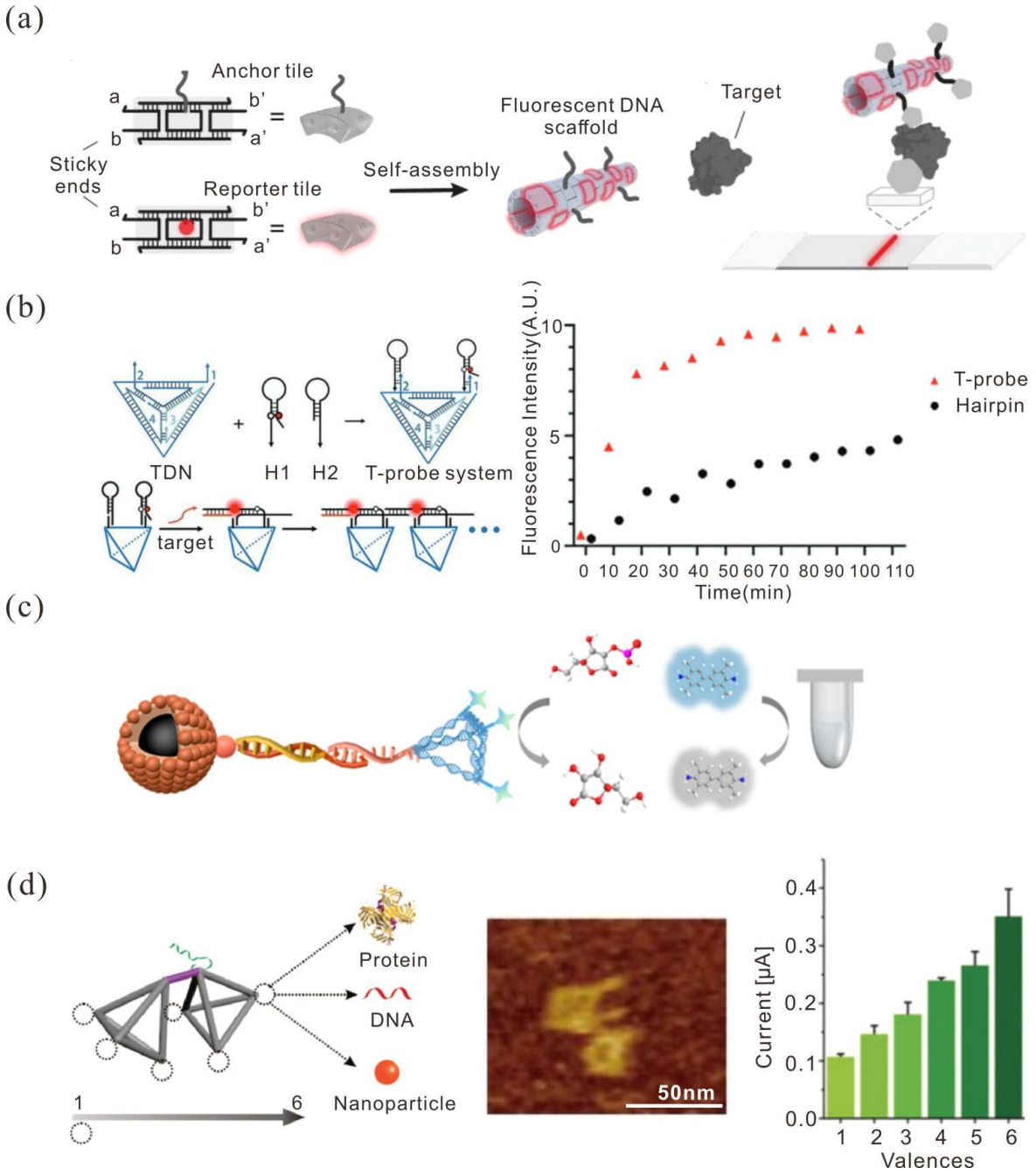

Figure 4. Signal Probes on DNA frameworks. **(a)** DNA tile-based scaffolds as functional reporters in lateral flow assays. Reprinted with permission [96]. Copyright 2023 Wiley-VCH GmbH; **(b)** Hairpin with fluorophore/quencher on TDF for HCR signal amplification. Reprinted with permission [98]. Copyright 2022 Wiley-VCH GmbH; **(c)** TDF-enabled multivalent ALP anchoring for signal-on PSA detection. Reprinted with permission [99]. Copyright 2025 American Chemical Society; **(d)** Valency-controlled signal amplification based on DNA frameworks. Reprinted with permission [28]. Copyright 2018 Wiley-VCH GmbH.

To achieve precise signal amplification, Liu *et al*. exploited valency-controlled enzyme recruitment for signal amplification. They constructed di-TDF assemblies that enabled stoichiometric recruitment of signaling molecules, with defined valencies from 1 to 6 [28]. When applied to electrochemical detection of circulating free DNA, the recruited horseradish peroxidase (HRP) catalyzed the 3,3',5,5'-Tetramethylbenzidine (TMB)-H_2O_2 reaction, generating amplified electrochemical signals

(Figure 4d). This dual amplification strategy enhanced sensitivity by 3–5 orders of magnitude and expanded the dynamic range from 3 to 5 orders of magnitude. In a related effort, Yin *et al*. developed programmable atom-like nanoparticle reporters by assembling DNA tetrahedral framework dimers [101]. This design allowed precise control over HRP valencies from 1 to 6 and enabled programmable signal amplification for multiplexed biomarker detection and accurate cancer diagnosis.

3. DNA framework-based pathogen detection methods

The functionalization strategies of DNA frameworks naturally translate into diverse detection approaches, differing primarily in their signal readout mechanisms. Electrochemical detection, which is well-suited for applications demanding high-sensitivity quantification and convenient electronic signal output, typically employs frameworks functionalized with redox-active probes or enzyme labels and anchored onto electrode surfaces to facilitate efficient electron transfer upon target recognition [102,103]. Fluorescence detection excels in providing spatially resolved imaging and visualization of dynamic conformational changes, relying on frameworks configured with precisely spaced fluorophore-quencher pairs or conformationally switchable probes for real-time optical readout of molecular interactions [104]. This functional diversity gives rise to the three major categories of DNA framework-based pathogen detection methods, electrochemical, fluorescence, and point-of-care testing (POCT) approaches, which are surveyed in the following sections.

3.1. Electrochemical methods

Electrochemical detection methods offer distinct advantages in the field of pathogen nucleic acid detection, due to their high sensitivity, fast response, low cost, and ease of integration and miniaturization [105,106]. To address the limitation of poor accessibility of Cas proteins to probes immobilized on heterogeneous electrode interfaces, Ding's group integrated a TDF with the cis and trans-cleavage activities of CRISPR-Cas12a to construct an electrochemical platform for amplification-free detection of human papillomavirus (HPV)-16 DNA [107]. Three thiol groups vertically immobilized the TDF on a gold nanoflower-modified carbon electrode, with a biotinylated reporter probe extending from the remaining vertex. When HPV-16 DNA is present, Protospacer Adjacent Motif (PAM) recognition and CRISPR RNA (crRNA) matching sequentially activate Cas12a cleavage, releasing the biotinylated probe from the electrode and reducing the streptavidin-horseradish peroxidase (SA-HRP)-mediated electrochemical signal. Compared with ssDNA probe-modified electrodes, the oriented TDF arrangement improved probe density and orientation, reduced interfacial crowding, and enhanced Cas12a cleavage efficiency at the solid–liquid interface.

In a subsequent study, Li and colleagues extended different numbers of reporter probes from the four vertices of a TDF to construct framework hotspot reporters with increasing local densities [108]. This design improved spatial accessibility and trans-cleavage efficiency of CRISPR-Cas12a, achieving target detection within 15 minutes with a sharp decrease in electrochemical current (Figure 5a). By simply changing the crRNA, amplification-free detection of various viral nucleic acids could be achieved. Hao *et al*. combined the use of TDFs with CRISPR-Cas12a for the electrochemical detection of parvovirus B19 DNA [109]. In this design, all four vertices of the TDF were modified with biotinylated reporter probes to achieve a high-density multivalent configuration. Once Cas12a is activated by the target, the

biotinylated probes were cleaved, preventing the subsequent binding of SA-HRP. The remaining SA-HRP on the electrode catalyzed the H_2O_2/hydroquinone redox reaction, producing an electrochemical signal that decreased with increasing target concentration. Additionally, they noted a size-matching effect between the 12 nm TDF and the Cas12a-crRNA complex (10–12 nm), which may facilitate efficient contact between Cas12a and the TDF on the electrode. This method achieved a detection limit of 2.19 fM.

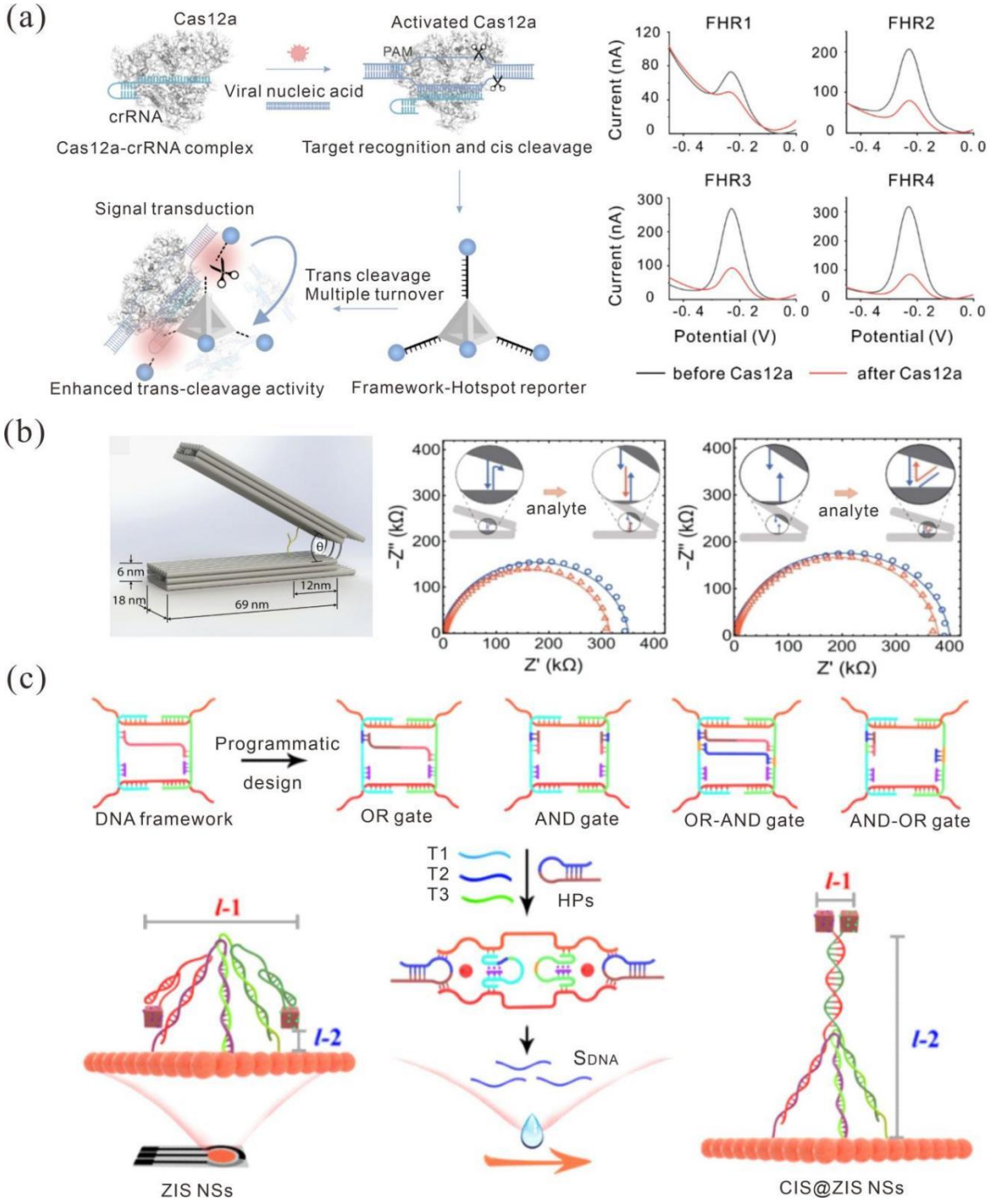

Figure 5. Electrochemical biosensors for pathogen detection based on DNA frameworks. **(a)** Methylene blue-labeled TDF hotspot reporters for viral nucleic acid detection. Reprinted with permission [108]. Copyright 2023 Wiley-VCH GmbH; **(b)** DNA origami hinge-based signal amplifier for electrochemical biosensing. Reprinted with permission [110]. Copyright 2025 Royal Society of Chemistry; **(c)** Programmable DNA framework-based logic-gated dual-distance regulation for photoelectrochemica sensor of Waterborne Viruses. Reprinted with permission [111]. Copyright 2026 American Chemical Society.

Although the electrochemical strategies combining TDF with CRISPR-Cas12a have improved sensitivity, they still suffer from several drawbacks, including reliance on enzymatic catalysis and sensor irreversibility. To overcome these limitations, Majikes *et al*. constructed a DNA origami hinge structure as a voltage-tunable signal amplifier [110]. Target binding induces conformational changes of the hinge, which directly alter the electrode capacitance, achieving approximately 20,000-fold signal amplification under direct current bias regulation with a detection limit below 1 fM, and also enabling sensor regeneration via strand displacement (Figure 5b). This approach advances single-target detection by redefining DNA nanostructures from passive scaffolds as active signal-processing elements. However, single-target detection modes are inadequate for multiplex differentiation given that clinical infections often involve multiple pathogens. To address this challenge, Chen and colleagues developed a programmable DNA framework-based logic-gated dual-distance regulation photoelectrochemical (PEC) sensor for the multiplex detection of waterborne viruses [111]. Target DNA triggers a conformational change in the framework, which activates a DNAzyme that cleaves a hairpin probe to release a signaling DNA strand (S_{DNA}). On one hand, the S_{DNA} moves Cu_2O nanoclusters (Cu_2O NCs) away from the $ZnIn_2S_4$ surface, disrupting the S-type heterojunction and restoring the photocurrent. On the other hand, it brings two types of Cu_2O nanoclusters into close proximity, enabling synergistic catalysis between their loaded glucose oxidase and HRP, releasing Cu^{2+} ions that react with $ZnIn_2S_4$ to form $CuIn_2S_4$. This establishes a type-II heterojunction that promotes electron–hole separation, with target quantification achieved by measuring the current intensity. Using DNA sequences of norovirus, rotavirus, and hepatitis A virus as targets, the researchers constructed AND, OR, AND–OR, and OR–AND logic gates, enabling parallel detection of multiple virus types in a single sample with a detection limit as low as 7.7 fM (Figure 5c). This work highlights the unique advantages of DNA frameworks in multiplexed signal transduction and pathogen detection in complex environments.

3.2. Fluorescence methods

Fluorescence signal is a typical readout method in the field of optical biosensors. Owing to its excellent sensitivity, molecular specificity and non-invasiveness, fluorescence enables the detection of various targets through diverse signal transduction mechanisms, such as FRET and fluorescence polarization (FP) [112]. Building on this principle, researchers have developed a series of DNA framework-based fluorescence sensing platforms for pathogen detection.

Chauhan and colleagues designed a net-shaped DNA nanostructure-based fluorescence turn-on sensor for SARS-CoV-2 detection [113]. In this design, three FAM-labeled aptamers were arranged in trimeric clusters on each vertex of 2 × 2, 3 × 3, and 4 × 4 DNA rhombus nets (constructed using a 42 bp triangle as the basic unit), with each aptamer partially hybridized with a BHQ1-labeled lock DNA to initially quench the fluorescence. The intra-cluster spacing of the three aptamers was 6 nm, precisely matching the distance between the three spike proteins within the SARS-CoV-2 spike trimer, while the inter-vertex spacing of 15 nm aligned with the inter-spike trimer distance on the viral surface. When target binding occurred, the spike proteins displaced the lock DNA, turning on the fluorescence signal. The 4 × 4 DNA net was validated as the optimal sensor, achieving a limit of detection of 1000 viral genome copies/mL in artificial saliva within 10 minutes at room temperature (Figure 6a).

To further enhance deformability to fit the spherical viral surface, Wang's team introduced a bioinspired design, extending the architecture from 2D grids to 3D dynamic structures [114]. Inspired

by human hands and bird claws, they designed a DNA NanoGripper comprising a palm and four bendable fingers, each with phalanges connected by rotatable joints. Fifty-two virus-binding aptamers were uniformly hybridized to ssDNA overhangs on the inner surfaces of the four fingers. The lock DNA (BHQ1) was partially complementary to the aptamer (FAM), and viral binding displaced the lock DNA, generating a fluorescent signal (Figure 6b). The DNA NanoGripper improved signal detection through a ssDNA anchor at the palm bottom for attachment to a photonic crystal surface, allowing digital counting of individual fluorescent spots from single viruses and reducing the detection limit from 1000 to 100 copies/mL. Additionally, its four fingers bend independently to actively grasp viral particles, enabling efficient wrapping of viruses with varying sizes or uneven spike distributions. Most fluorescence methods operate in a "signal-on" mode, which often suffers from high background interference. In contrast, the "signal-off" mode offers advantages in specific scenarios, such as complex biological matrices [77,115]. Wei *et al*. combined CRISPR/Cas12a trans-cleavage with enzyme-catalyzed click chemistry to design an methicillin-resistant *Staphylococcus aureus* (MRSA)-induced fluorescence "turn-off" sensing platform [116]. They embedded four CLICK-17 DNAzymes into a rigid tetrahedral framework to construct a bifunctional FNAzyme, while magnetic nanoparticle-conjugated MRSA-specific aptamers recognized the target. Bacteria-aptamer binding released activators, and the activated Cas12a/crRNA complex cleaved the CLICK-17 DNAzymes, blocking the click reaction and turning off the fluorescence signal. This technology achieved a fluorescence "on-to-off" transition and detected MRSA as low as 18 CFU/mL, a 54-fold improvement over conventional methods.

Unlike intensity-based fluorescence measurements, FP is a ratiometric technique that is less affected by fluorophore concentration and excitation intensity fluctuations, offering a more stable readout in homogeneous assays. Zhang *et al*. extended DNA frameworks-based fluorescence sensors to bacterial detection by introducing FP technology. They constructed a 2D DNA monolayer via self-assembly of double-stranded DNA tiles, anchoring *Salmonella* hairpin aptamers (HAPs) to the monolayer surface [117]. *Salmonella* first triggered circular isothermal strand displacement amplification (CSDA), which dissociated the HAPs from the monolayer and exposed the δ sites, allowing numerous 5'-FAM-labeled reporting probes (RP^{FAM}) to be enriched on the monolayer through δ site hybridization. As RP^{FAM} transitioned from a free state to a constrained state, FAM rotation was restricted, leading to an increased FP value (Figure 6c). This study introduced FP technology, in which CSDA synergized with the large-area flexible monolayer to enrich RP^{FAM}, converting a low FP background into a high FP output, with the FP increase proportional to bacterial concentration. Compared with fluorescence intensity, FP avoids quenching issues. The multivalent enrichment of the large-area DNA monolayer and the cyclic amplification of CSDA significantly enhanced the FP signal, enabling detection of *Salmonella* as low as 7.2 CFU/mL. Rather than relying on target-induced FP changes, Huang *et al*. exploited DNA frameworks to construct stable fluorescence anisotropy (FA) barcodes for multiplexed detection [118]. By precisely positioning fluorophores at specific locations of TDFs, they generated distinct and programmable FA values serving as identification tags. Each FA barcode was conjugated with a specific recognition probe, enabling simultaneous detection of multiple nucleic acid targets (Figure 6d). In this platform, the FA value identifies the target type, while the fluorescence intensity correlates with target concentration for quantification. This strategy can be readily adapted for multiplexed pathogen detection by substituting the recognition probes with pathogen-specific sequences. To achieve FA-based signal amplification, Xie *et al*. designed an

octopus-like DNA nanostructure coupled with graphene oxide for dual FA enhancement. In this assay, the authors achieved a detection limit of 330 pmol/L for hepatitis B virus DNA [119].

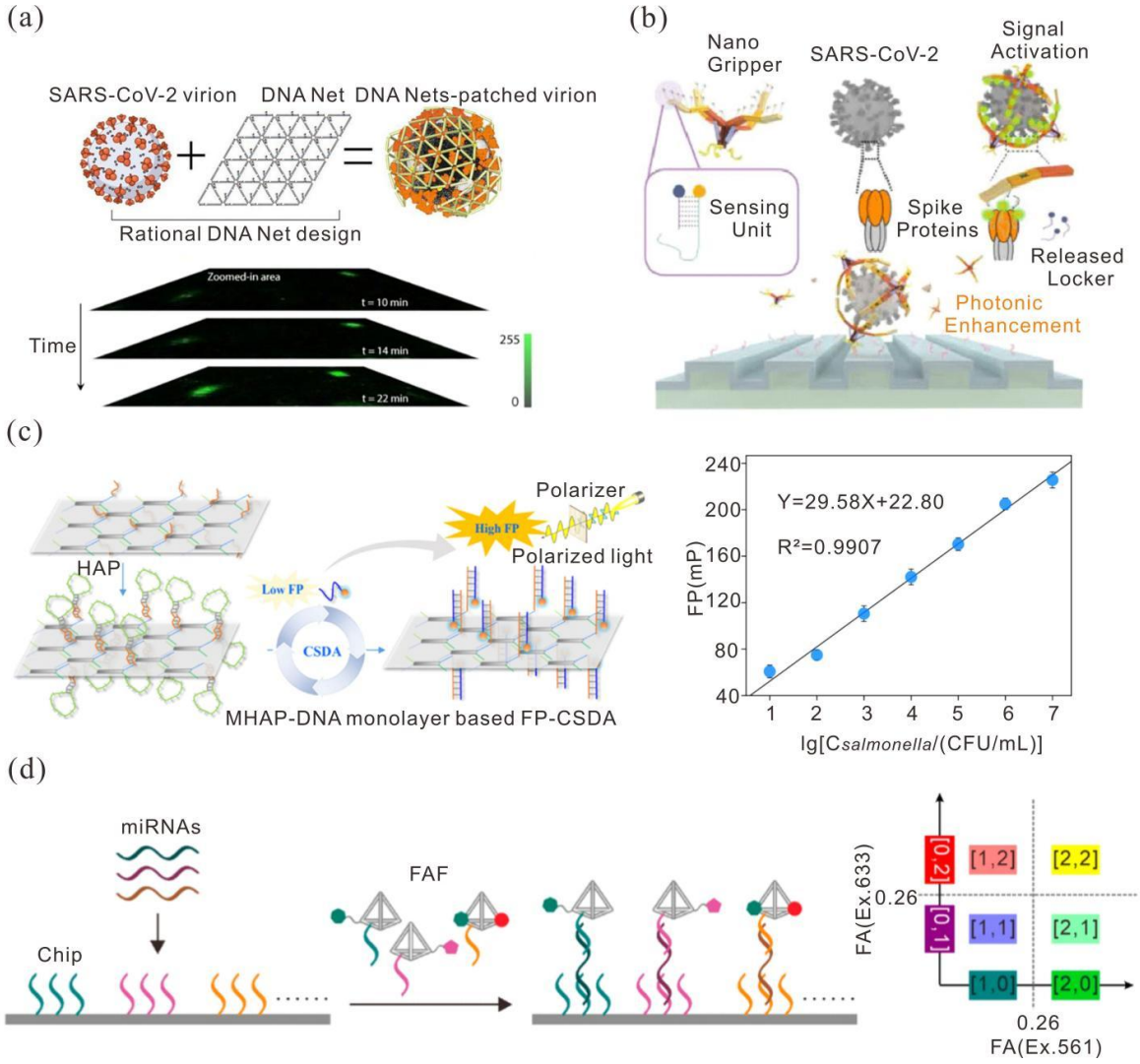

Figure 6. DNA frameworks-based fluorescent biosensors for pathogen detection. **(a)** Net-shaped DNA nanostructure with aptamer switches for fluorescence turn-on detection of SARS-CoV-2. Reprinted with permission [113]. Copyright 2023 American Chemical Society; **(b)** Aptamer-switched fluorescence activation of DNA nanoGripper for SARS-CoV-2 detection. Reprinted with permission [114]. Copyright 2024 American Association for the Advancement of Science; **(c)** Fluorescence polarization-responsive DNA monolayer platform for Salmonella sensing. Reprinted with permission [117]. Copyright 2023 American Chemical Society; **(d)** Fluorescence Anisotropy Barcodes for Multiplexed Analysis. Reprinted with permission [118]. Copyright 2021 American Chemical Society.

3.3. POCT methods

POCT devices offers distinct advantages over traditional laboratory-based methods, including portability, ease of operation by non-professionals, and rapid on-site results, making it highly promising for applications in food safety, environmental monitoring, and healthcare [120,121].

Recently, Xiao *et al*. innovatively developed a smartphone-based fluorescence/ colorimetric dual-mode sensor for the on-site detection of *Salmonella* [122]. In this platform, a TDF-based multivalent aptamer binds to the target bacteria and releases complementary DNA strands, triggering catalytic hairpin assembly (CHA) and generating both fluorescence and colorimetric signals. A 3D-printed dark chamber provides a closed and controllable illumination environment, while a smartphone captures the images and a WeChat mini-program automatically analyzes the signal to determine the bacterial concentration (Figure 7a). This method achieves a detection limit as low as 10 CFU/mL with a single-test cost of approximately 2 RMB. Chen *et al*. further developed a self-powered dual-mode sensing chip that converts biorecognition events into measurable electrical signals using an enzymatic biofuel cell [123]. This platform wirelessly transmits electrochemical signals to a smartphone or allows colorimetric readout by the naked eye, enabling the detection of *Pseudomonas aeruginosa* (*P. aeruginosa*) as low as 0.83 CFU/mL. Du's group integrated a TDF-based sensing interface with the CRISPR/Cas12a system and HCR to invent a portable electrochemical biosensor for the ultrasensitive detection of monkeypox virus (MPXV) [124]. An HCR initiator chain extended from the TDF vertex served as the cleavage switch for Cas12a. When activated by MPXV DNA, Cas12a cleaved the initiator chain and blocked HCR on the electrode surface. In the absence of MPXV DNA, the intact initiator chain triggered HCR, anchoring HRP onto the electrode to catalyze the TMB-H_2O_2 reaction and generate a current signal (Figure 7b). Using a screen-printed carbon electrode, a portable electrochemical reader, and a mobile phone application, this platform achieved a detection limit of 194.48 aM in 10% human saliva.

To achieve the detection of drug-resistant bacteria, Yaadav and colleague developed a DNA origami nanoantenna platform for single-molecule detection of carbapenem-resistant *K. pneumoniae*. The core of this platform is a 3D DNA origami structure termed the "Trident", whose two side pillars anchor two silver nanoparticles to form a plasmonic "hotspot" [125]. Capture strands extended within the hotspot region allow the target gene to bridge the capture strand and a fluorescent reporter strand, positioning the fluorophore at the center of the hotspot. This configuration enhances the fluorescence signal several thousand-fold, which is directly captured by a compact fluorescence reader. Combined with nanosphere lithography and microfluidic technology, the Trident structures are densely immobilized on a glass surface for efficient target enrichment (Figure 7c). The platform detects as low as 5 aM of target nucleic acid (the OXA-48 gene, a specific biomarker of this drug-resistant bacterium) within one hour, enabling accurate screening of drug-resistant strains from mixed samples. For further multi-target detection, Dou and coworkers developed a smartphone-based "three-in-one" electrochemical biosensor from the perspective of comprehensive clinical information [126]. This sensor simultaneously achieves femtomolar-level detection of SARS-CoV-2 RNA, S protein, and S protein antibody on a single chip, enabling comprehensive tracking of patients from infection to immunization.

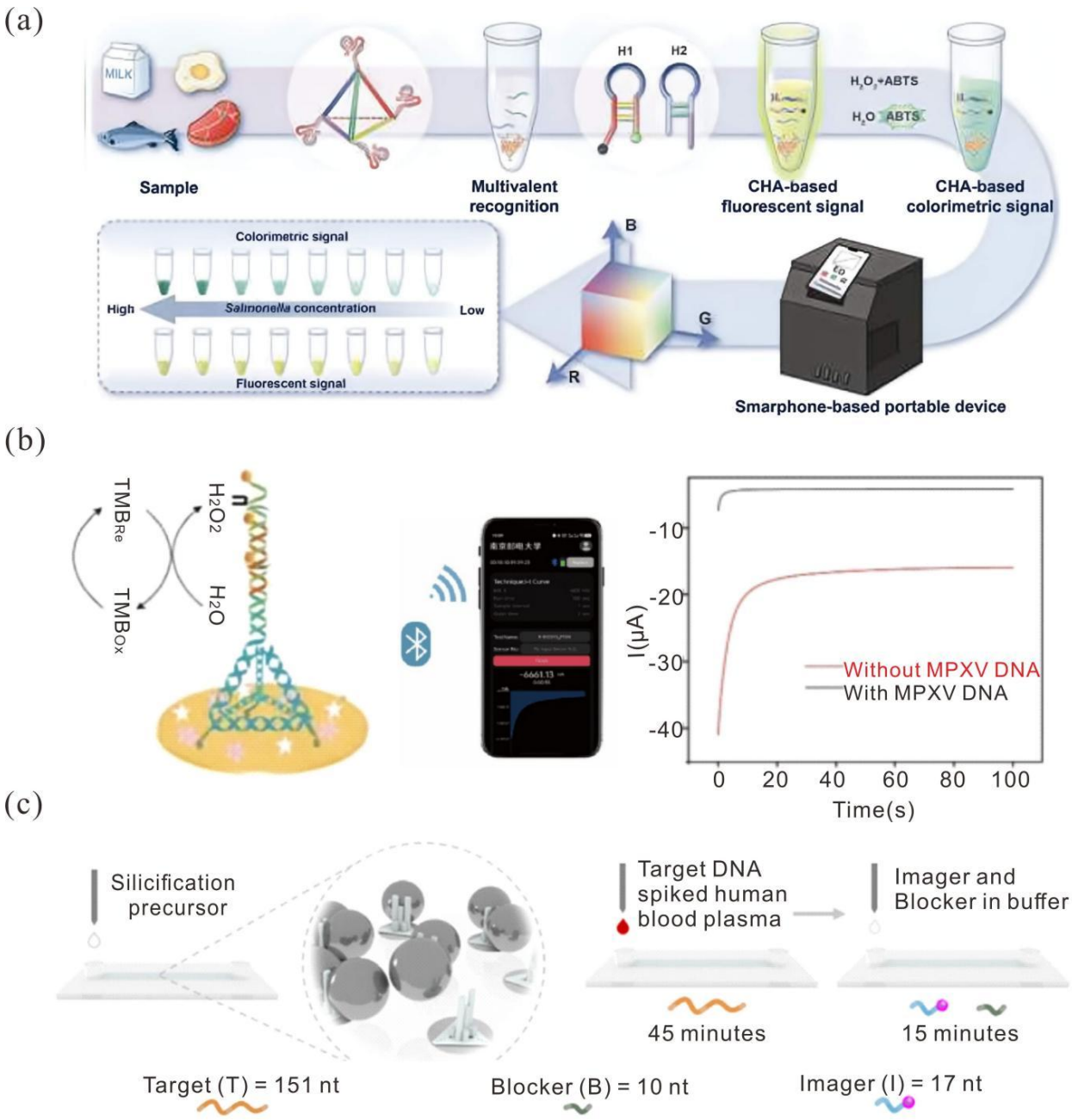

Figure 7. DNA frameworks-based POCT biosensors for pathogen detection. **(a)** Smartphone-based fluorescence/colorimetric dual-mode POCT platform for Salmonella detection. Reprinted with permission [122]. Copyright 2025 American Chemical Society; **(b)** TDF-mediated CRISPR/HCR amplification strategy with smartphone-based electrochemical readout for MPXV. Reprinted with permission [124]. Copyright 2026 Elsevier; **(c)** Trident DNA origami nanoantenna array for sandwich-hybridization detection of nucleic acids. Reprinted with permission [125]. Copyright 2025 Wiley-VCH GmbH.

To provide a more intuitive comparison of analytical performance across different detection platforms, we summarize the key metrics of conventional methods and representative DNA framework-based sensors in Table 1, including LOD, dynamic range, test duration, and target type. The optimal choice among these sensors should be determined by the specific requirements of each application scenario, balancing sensitivity, throughput, speed, portability, cost, and operational complexity.

Table 1. Comparison of analytical performance between conventional methods and DNA framework-based sensors for pathogen detection.

Method	Representative technique	Target type	Limit of detection	Dynamic range	Test duration
Microbial culture	Plate counting /Enrichment	Bacteria	30 CFU/mL	/	5–7 days
Immunoassay	ELISA	Proteins/whole bacteria	10^3–10^5 CFU/mL	/	2–4 h
Molecular Biology	qPCR	Nucleic acids	10–100 copies/μL	/	1–3 h
	Metagenomic sequencing	Nucleic acids	10–10^3 copies/μL	/	24 h
MS	MALDI-TOF MS	Protein	10^4–10^5 CFU/mL	/	< 1 h
DNA framework-based sensors	TDF-enhanced CRISPR-Cas12a electrochemical sensor [108]	SARS CoV-2 pseudovirus particles, HPV DNA, HBV DNA	SARS CoV-2: 100 TU/μL; HPV: 1 pM; HBV: 100 fM	200–4000 TU/μL	15 min
	DNA logic gates-based DNA sensor [111]	norovirus, rotavirus, and hepatitis A virus DNA	7.7 fM	0.001–500 nM	1.5–3.5 h
	Net-shaped DNA sensor [113]	SARS-CoV-2 virions	~1000 viral genome copies/mL	1×10^4–1×10^{10} copies/mL	10 min
	DNA NanoGripper-based biosensor [114]	SARS-CoV-2 virions	~100 copies/mL	10^2–10^7 copies/mL	30 min
	DNA monolayer-based FP sensor [117]	*Salmonella*	7.2 CFU/mL	10–10^7 CFU/mL	45 min
	DNA origami nanoantenna-based sensor [125]	*K. pneumoniae*	5 aM	1 aM–5 nM	60 min
	TDF-based fiber-optic SPR sensor [127]	N protein of SARS-CoV-2	34 nM	0.2–2.5 μM	25 min
	Star-shaped DNA sensor [128]	Dengue virion	1×10^2 p.f.u./mL in human serum; 1×10^3 p.f.u./mL in plasma	10^2 p.f.u./ml–10^5 p.f.u./mL	1–2 min
	DNA nanosphere-based ECL sensor [129]	*S. aureus*, MRSA, *P. aeruginosa*, *K. pneumoniae*	10^2 CFU/mL	10^2–10^6 CFU/mL	45 min
	DNA-encoded microsphere-based sensor [130]	*S. aureus*, *E. coli*, *Salmonella typhimurium*, *Listeria monocytogenes*	39–101 CFU/mL	10^2–10^8 CFU/mL	1.5 h

Abbreviations: qPCR: quantitative real-time polymerase chain reaction; MALDI-TOF MS: Matrix-Assisted Laser Desorption/Ionization Time-of-Flight Mass Spectrometry; SPR: Surface Plasmon Resonance; ECL: electrochemiluminescence; *E. coli*: *Escherichia coli*.

4. Applications of DNA frameworks in pathogen detection

Drawing on the design principles outlined above, DNA frameworks-based sensors have been extensively applied to detect viruses and bacteria in both clinical and environmental samples. In this section, we will introduce their specific applications according to different target types.

4.1. Virus detection

Based on the type of biomarker, viral detection strategies can be categorized into protein detection and nucleic acid detection. Pin *et al*. immobilized a TDF-aptamer conjugate on the surface of a plasmonic tilted fiber Bragg grating sensor [127]. Target capture-induced changes in the surface refractive index led to a red shift in the resonance wavelength, enabling label-free, real-time quantitative detection of the SARS-CoV-2 nucleocapsid (N) protein. Spiking experiments in artificial saliva (0.6 μM N protein) validated the sensor's feasibility in complex matrices, with a response time of approximately 25 minutes. After regeneration with 1% sodium dodecyl sulfate, the sensor retained over 97% of its initial signal over three cycles (Figure 8a). Targeting internal components of virus typically requires heat inactivation of the sample, making the procedure relatively cumbersome. In contrast to this strategy, Lorenzo's group focused on a surface protein target and developed an electrochemical aptasensor based on a bismuthene-DNA tetrahedron nanobioconjugate for the detection of the SARS-CoV-2 spike (S1) protein [131]. The sensor showed a linear detection range from 10 fg/mL to 1 pg/mL, with a detection limit as low as 1.74 fg/mL. Recovery experiments were performed by spiking authentic nasopharyngeal swab samples with S1 protein at concentrations of 50.0 fg/mL and 100 fg/mL, yielding recoveries of 115% and 122%, respectively. In contrast, the same samples tested with a commercial rapid antigen test gave negative results, demonstrating that the sensitivity of this sensor outperforms commercially available antigen detection methods.

While the above strategies target individual protein biomarkers, some viruses present geometrically arranged antigen clusters that enable multivalent recognition. The envelope protein domain III (ED3) of dengue virus (DENV) exhibits an icosahedrally symmetric arrangement, forming trivalent and pentavalent antigen clusters spaced approximately 14–15 nm apart, providing an ideal target for direct virus capture based on spatial pattern matching. Accordingly, Kwon *et al*. designed a star-shaped DNA scaffold assembled via DNA tile-based self-assembly, in which the ten vertices extending aptamers precisely match the geometric pattern formed by the ED3 clusters [128]. The target pulls apart the molecular beacon-like structures (FAM/BHQ1) on the inner edges, resulting in fluorescence recovery (Figure 8b). Human serum samples containing different concentrations of DENV were tested using this method alongside gold-standard methods (RT-PCR and ELISA). The sensor exhibited an excellent limit of detection of 10^2 PFU/mL, outperforming the 10^3 PFU/mL achieved by RT-PCR.

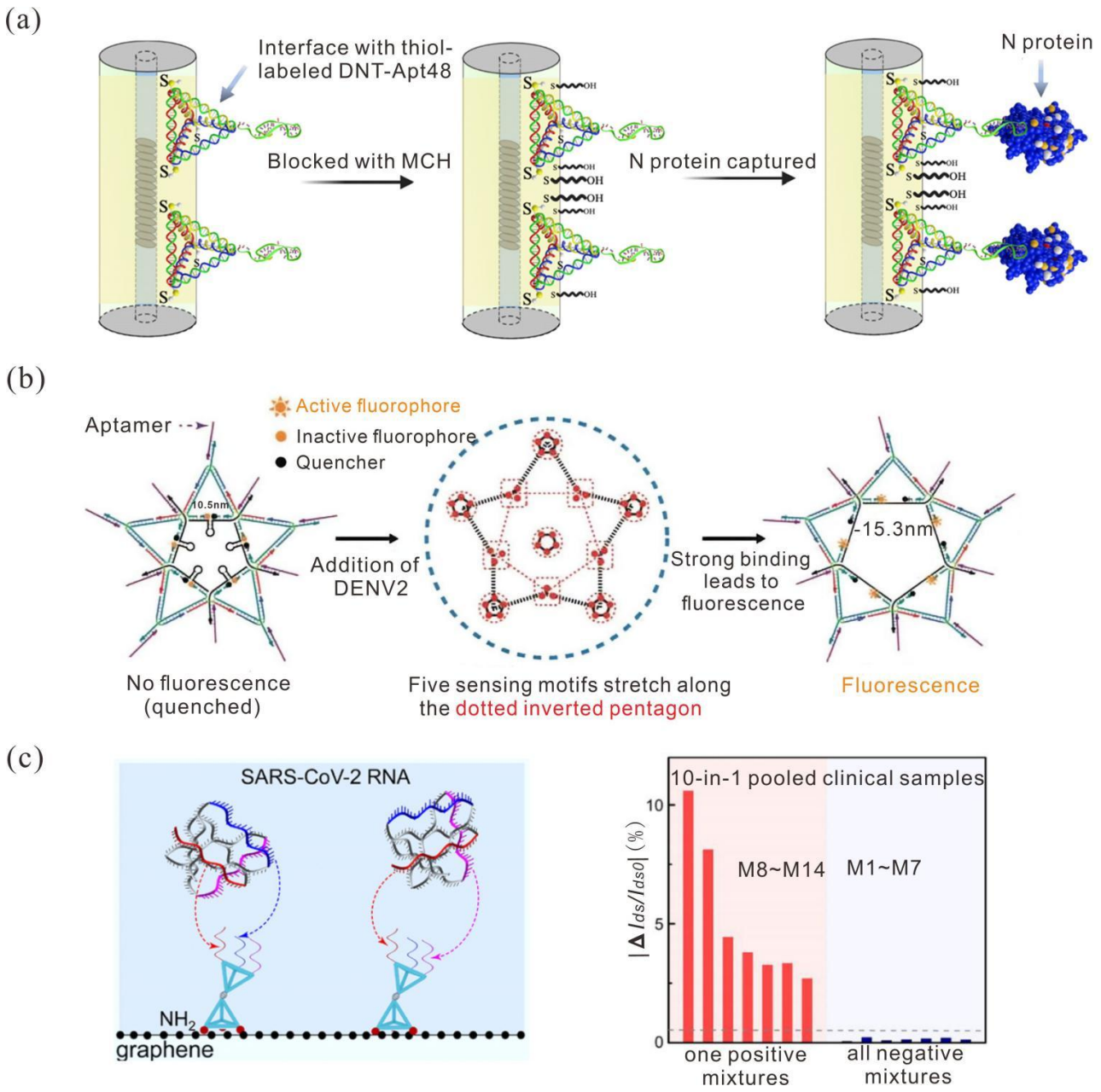

Figure 8. Virus detection applications based on DNA frameworks. **(a)** DNA tetrahedron-assisted oriented immobilization of aptamers on fiber-optic SPR biosensor for COVID-19 biomarker detection. Reprinted with permission [127]. Copyright 2026 Springer Nature; **(b)** Star-shaped DNA framework for multivalent spatial pattern-matching-based detection of DENV. Reprinted with permission [128]. Copyright 2019 Springer Nature; **(c)** TDF dimer-based transistor sensor for SARS-CoV-2 pooled testing. Reprinted with permission [132]. Copyright 2022 American Chemical Society.

In addition to viral protein detection, nucleic acid-based strategies offer high specificity for viral diagnosis. Min *et al*. developed an electrochemical biosensor based on a floating-gate carbon nanotube field-effect transistor (FET) capable of effectively identifying a single positive sample within a 10-in-1 pooled sample [133]. This platform enabled respiratory syncytial virus RNA detection within 40 seconds at a detection limit as low as 0.1 copies/μL. In 20 clinical nasopharyngeal swab samples, the sensor correctly identified all 10 positive cases and exhibited a cross-reactivity below 4% with other

viruses. However, pooled testing often suffers from reduced sensitivity and specificity due to target dilution or sample contamination. To resolve this problem, Wu *et al*. developed a graphene FET sensor modified with a triple-probe TDF dimer, achieving ultrasensitive 10-in-1 pooled detection of SARS-CoV-2 RNA with a detection limit of 0.025–0.05 copies/μL [132]. In 30 nasopharyngeal swab samples, the sensor accurately identified all 14 positive cases, showed complete concordance with RT-PCR results (specificity of 1.00), and achieved an average diagnosis time of 74 seconds per sample. For 14 pooled samples, the 7 pools containing positive samples yielded response signals of 27%–53%, while the 7 all-negative pools produced signals of only –2% to 2% (Figure 8c). For multiplex detection of multiple viral targets, Zhan *et al*. developed a method combining TDF-enhanced CRISPR-Cas12a with inductively coupled plasma mass spectrometry for simultaneous detection of HPV-16, HPV-18, and HPV-52 [134]. Testing of 15 cervical swab samples showed complete concordance with DNA sequencing. Spike recovery experiments in diluted serum achieved rates of 90.7%–112.7% for the three targets. With a detection limit of 218 fM, this method provides a reliable tool for early cervical cancer screening and HPV genotyping.

4.2. Bacteria detection

Bacteria possess a complete cellular structure, larger dimensions, and more complex surface antigens, which impose higher demands on the sensing interface in terms of recognition efficiency and anti-interference capability. Moreover, bacterial infections often involve mixed infections of multiple pathogens, presenting additional challenges for the multiplexing capacity of detection methods [135]. Accordingly, various DNA frameworks-based sensors have been developed for authentic clinical, environmental, and food samples. The following sections focus on analytical platforms targeting intact bacteria and bacterial lysates.

Tang and colleagues designed a fluorescent nanoprobe based on TDF-supported HCR for in situ analysis of *S. aureus*. The probe specifically binds to bacteria through dual recognition by an antibody and an aptamer, triggering simultaneous HCR at three vertices of the tetrahedron and achieving efficient fluorescence signal amplification. This method achieves a detection limit of 26 CFU/mL. When *S. aureus* was spiked into cancer cell lysate and fetal bovine serum, the fluorescence signals showed no statistical difference from those in PBS buffer, demonstrating good tolerance in complex biological matrices [136]. To further improve detection sensitivity, Wang *et al*. constructed a DNA nanotree on an FET surface, featuring an RNA-cleaving DNAzyme as the trunk and Y-shaped branches as the canopy. The sensor exhibited a linear detection range of 1–10^5 CFU/mL for *S. aureus* and could detect as low as 1 CFU/mL within 5 minutes. Recoveries ranging from 91.33% to 109.41% were obtained by spiking *S. aureus* at different concentrations (10^2, 10^3, and 10^4 CFU/mL) into lake water, milk, and juice samples [137]. This work highlights the unique advantages of short-chain self-assembled DNA frameworks in constructing low-cost, highly sensitive bacterial sensors.

To achieve multiplex detection, Zhang *et al*. developed an ECL sensor based on a DNA helical nanosphere integrated with a microfluidic chip for simultaneous detection of four pathogens [129]. The nanosphere is locked by aptamers and opens following target capture, releasing encapsulated luminophores and amplifying the ECL signal via nanoceria electrocatalysis (Figure 9a). Tested on 27 clinical samples (urine, blood, pleural/peritoneal effusion), the sensor showed high concordance with digital PCR (Spearman correlation > 0.99) and 100% accuracy within 45 minutes. Whereas

Zhang's strategy relies on the physical release of sequestered signal molecules upon nanostructure disassembly, Wang *et al*. developed a "signal retention" platform in which fluorescent probes are pre-anchored onto the surface of encoded microspheres, and target recognition leads to probe cleavage and detachment via enzyme-mediated digestion [130]. The platform achieved four-plex pathogen discrimination using two sizes and two colors. Notably, this 2D encoding library can be expanded by introducing additional sizes or colors of microsphere (Figure 9b). With a computer vision algorithm for automated counting, the platform achieved a detection limit of 100 CFU/mL. The platform was validated on 10 clinical and 10 fish samples, showing results consistent with plate counting and completing multiplex detection within 1.5 hours, far outperforming traditional culture (24–48 hours).

In addition to direct detection of intact bacteria, analyzing the internal components released after bacterial lysis can provide more precise species identification. The 16S rRNA sequence consists of alternating conserved and variable regions, with the variable regions being species-specific, making it an ideal target for bacterial discrimination. Depending on the detection target, methods can be divided into 16S rRNA gene detection and 16S rRNA detection. Tang *et al*. designed a dual-recognition fluorescent sensor based on TDF-supported click ligation for highly specific detection of the *P. aeruginosa* 16S rRNA gene [138]. The sensor utilizes two vertex probes on the TDF to simultaneously recognize two distinct regions of the 16S rRNA gene, effectively avoiding false positives caused by nonspecific binding of single probes. Spiking tests in fetal bovine serum and urine showed no significant difference from PBS buffer, with a detection limit of 151 CFU/mL. For multiplexed bacterial discrimination via 16S rRNA, Li's group employed a triangle DNA origami-based positional encoding digital recorder to achieve multiplex bacterial discrimination through 16S rRNA detection [139]. The platform immobilizes specific probes at six distinguishable positions on the triangle DNA framework. Target sequences are recognized through a sandwich hybridization mechanism, wherein they bridge probes and biotinylated reporters. The resulting complexes are then decorated with streptavidin and imaged by AFM, allowing for the positional readout of bacterial types based on the spatial distribution of bright spots. By trimerizing the framework, the detection throughput can be expanded to 18 bacteria (Figure 9c). They applied this platform to drinking water and river water samples, the signals of *E. coli* were both significant in drinking water exposed for 20 days and river samples. They also collected soil near medical waste and found *E. coli* and *Lactobacillus* simultaneously, with recording efficiencies of approximately 79.1% and 72.1%, respectively. These findings were consistent with qPCR results. This work provides a fluorescence-free, high-throughput tool for environmental microbial monitoring.

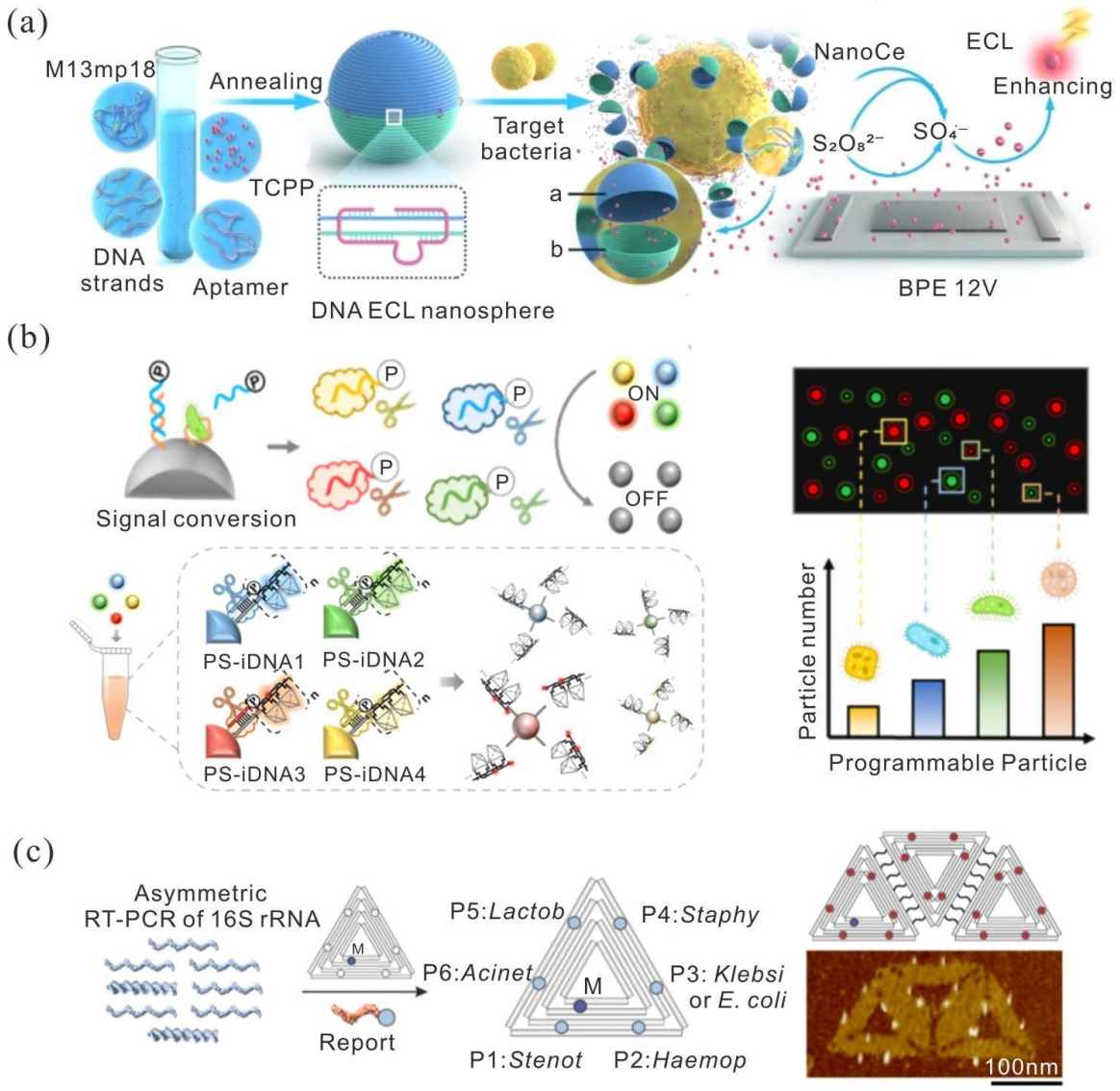

Figure 9. Bacteria sensing applications based on DNA frameworks. **(a)** DNA helical nanosphere-based "Off-On" ECL sensor for bacterial detection. Reprinted with permission [129]. Copyright 2025 American Association for the Advancement of Science; **(b)** Fluorescent microsphere-encoded multiplex bacterial detection. Reprinted with permission [130]. Copyright 2025 American Chemical Society; **(c)** DNA framework-encoded digital recorder for bacterial 16S rRNA recording and identification. Reprinted with permission [139]. Copyright 2026 American Chemical Society.

Beyond species identification, monitoring antibiotic resistance genes shed by bacteria into environmental waters is equally critical for public health surveillance. Liu *et al.* developed a TDF-based "Velcro" ECL sensor for the detection of the mecA gene of MRSA in environmental waters [140]. The TDF array provided effective shielding against bacterial invasion and enzymatic degradation in complex matrices, enabling sensitive detection with a limit of 2.3 fM. The sensor was validated in tap water, river water, and wastewater treatment plant effluent, with recovery rates ranging from 98.0% to 108.3%, demonstrating its practical applicability for environmental surveillance of antibiotic resistance genes.

5. Conclusions and perspectives

Over the past few decades, research on DNA frameworks for pathogen detection has advanced rapidly. Numerous research groups worldwide have developed ingenious sensing strategies to improve the speed, sensitivity, and portability of target detection. In this review, we mainly summarized the applications of DNA framework-based sensors for pathogen detection. The advantages of DNA framework for constructing pathogenic sensors are as follows. First, DNA frameworks are highly programmable. By designing framework nucleic acids with structural rigidity and controllable size, the spatial arrangement and orientation of probes can be precisely controlled, which significantly reduces steric hindrance during probe-target binding and improves target recognition capability. Second, DNA frameworks enable precise control over the number and spatial distribution of probes. Consequently, biosensors constructed on the basis of DNA frameworks can be used to investigate intermolecular interaction mechanisms at the single-molecule level. Third, the intrinsic addressability of DNA frameworks allows precise organization of signal molecules for efficient signal amplification. Furthermore, the favorable biocompatibility of DNA frameworks facilitates their direct application in biological samples with minimal toxicity or immunogenicity.

However, several limitations remain in the current application of DNA frameworks to pathogen sensing. First, the synthesis cost of functional DNA frameworks remains high, and complex framework nucleic acids suffer from low yield and structural instability. Therefore, there is an urgent need to optimize synthesis strategies to improve assembly yield and enhance the mechanical strength of DNA frameworks while maintaining structural precision. Silica mineralization offers a promising solution to this challenge [15,141–144]. Second, many sensors exhibit excellent detection performance for pathogens under laboratory conditions, but their feasibility and sensitivity often decline when applied to real biological samples (such as blood, saliva, or urine). An effective approach to address this challenge is to synthesize and screen efficient functional probes and to construct more stable DNA frameworks that are resistant to ionic strength, temperature, and nucleases, thereby maximizing probe protection [79,145]. UV-induced thymine dimerization, enzymatic ligation, and biomimetic mineralization have been explored to enhance the stability of DNA frameworks in complex biological matrices [146]. Enzymatic ligation covalently seals nicks within DNA frameworks but requires pre-phosphorylation and may restrict conformational flexibility [147], whereas calcium phosphate mineralization enhances nuclease resistance but suffers from limited thickness control and prolonged processing times [148]. Furthermore, combining DNA nanostructures with other nanomaterials, such as gold nanoparticles, graphene oxide, and quantum dots, can also help avoid false-positive signals caused by enzymatic degradation or interference from other molecules in bodily fluids. For instance, Wang *et al*. demonstrated that AuNP-deposited electrodes functionalized with TDF achieved attomolar-level detection of target DNA in serum with negligible signal interference [149]. Third, co-infections require the combined diagnosis of multiple markers. However, the design of DNA frameworks-based sensors capable of simultaneously targeting and detecting different targets remains limited. Although multiple fluorescent probes have been attached to DNA frameworks to achieve simultaneous detection of multiple bacteria or viruses, this approach is constrained by the fluorescence overlap of the limited number of available fluorescent dyes [150]. Therefore, biosensors with genuine multiplexing capability are urgently required. Fourth, the demand for on-site detection and large-scale screening of pathogens has also driven the emergence

of portable, point-of-care biosensors. Currently, preliminary efforts to address this challenge have utilized microfluidic chip technology and lateral flow assays [151,152]. Furthermore, with the widespread adoption of smart portable devices and advances in 3D printing technology, on-site colorimetric and electrochemical detection can be achieved without bulky instrumentation. This has effectively promoted the translation of DNA framework-based pathogen detection from laboratory settings to practical applications. With the continuous development of DNA nanotechnology and synthetic biology, researchers will continue to construct more sensitive and practical biosensing platforms, providing effective solutions for scientific questions and technical challenges.

Declaration of generative AI and AI-assisted technologies

During the preparation of this manuscript, the authors used generative AI tools only to improve language and readability. Specifically, the authors used ChatGPT and Deepseek for language polishing and for idea development in limited sections. The authors take full responsibility for the content of the manuscript.

Acknowledgments

This work was supported by the National Natural Science Foundation of China (No. 32471426).

Authors' contribution

Conceptualization, M.L. and L.L.; writing—original draft preparation, L.L. and L.S.; supervision, M.L. and L.S.; writing—review and editing, X.Z.; funding acquisition, M.L. All authors have read and agreed to the published version of the manuscript.

Conflicts of interest

Xiaolei Zuo holds the position of Editorial board member for *Life Analysis* and has not peer reviewed or made any editorial decisions for this paper. The authors declare no other conflicts of interest.

References

[1] Xu J, Akhtar M, Meng W, Bai J, Prince S, *et al.* Advances in pathogen detection: from traditional methods to nanotechnology, biosensing and AI integration. *Wiley Interdiscip. Rev. Nanomed. Nanobiotechnol.* 2025, 17(4):e70022.

[2] Salehi B, Abu-Darwish MS, Tarawneh AH, Cabral C, Gadetskaya AV, *et al*. Global burden of bacterial antimicrobial resistance in 2019: a systematic analysis. *Lancet* 2022, 399(10325):629–655.

[3] Nasrollahzadeh M, Sajjadi M, Soufi GJ, Iravani S, Varma RS. Nanomaterials and nanotechnology-associated innovations against viral infections with a focus on coronaviruses. *Nanomaterials* 2020, 10(6):1072.

[4] Cookson WO, Cox MJ, Moffatt MF. New opportunities for managing acute and chronic lung infections. *Nat. Rev. Microbiol.* 2018, 16(2):111–120.

[5] Rajapaksha P, Elbourne A, Gangadoo S, Brown R, Cozzolino D, *et al.* A review of methods for the detection of pathogenic microorganisms. *Analyst* 2019, 144(2):396–411.

[6] Zeng D, Chen Z, Jiang Y, Xue F, Li B. Advances and challenges in viability detection of foodborne pathogens. *Front. Microbiol*. 2016, 7:1833.

[7] Walter J, Eludin Z, Drabovich AP. Redefining serological diagnostics with immunoaffinity proteomics. *Clin. Proteom*. 2023, 20(1):42.

[8] Yang S, Rothman RE. PCR-based diagnostics for infectious diseases: uses, limitations, and future applications in acute-care settings. *Lancet Infect. Dis*. 2004, 4(6):337–348.

[9] Yalley AK, Ahiatrogah S, Kafintu-Kwashie AA, Amegatcher G, Prah D, *et al.* A systematic review on suitability of molecular techniques for diagnosis and research into infectious diseases of concern in resource-limited settings. *Curr. Issues Mol. Biol.* 2022, 44(10):4367–4385.

[10] Zhang YV, Rockwood A. Impact of automation on mass spectrometry. *Clin. Chim. Acta* 2015, 450:298–303.

[11] Goussarov G, Mysara M, Cleenwerck I, Claesen J, Leys N, *et al.* Benchmarking short-, long- and hybrid-read assemblers for metagenome sequencing of complex microbial communities. *Microbiology* 2024, 170(6):001469.

[12] Ge Z, Gu H, Li Q, Fan C. Concept and development of framework nucleic acids. *J. Am. Chem. Soc.* 2018, 140(51):17808–17819.

[13] Lin M, Wang J, Zhou G, Wang J, Wu N, *et al.* Programmable engineering of a biosensing interface with tetrahedral DNA nanostructures for ultrasensitive DNA detection. *Angew. Chem. Int. Ed.* 2015, 54(7):2151–2155.

[14] Veneziano R, Ratanalert S, Zhang K, Zhang F, Yan H, *et al.* Designer nanoscale DNA assemblies programmed from the top down. *Science* 2016, 352(6293):1534.

[15] Liu X, Zhang F, Jing X, Pan M, Liu P, *et al.* Complex silica composite nanomaterials templated with DNA origami. *Nature* 2018, 559(7715):593–598.

[16] Jones MR, Seeman NC, Mirkin CA. Programmable materials and the nature of the DNA bond. *Science* 2015, 347(6224):1260901.

[17] Ning Y, Li B, Chen W, Feng L, Huang X, *et al.* DNA framework-based lysosome-targeting chimeras: Intracellular ATP-facilitated extracellular protein degradation. *ACS Nano* 2025, 19(16):15853–15862.

[18] Zhou L, Yu B, Gao M, Chen R, Li Z, *et al.* DNA framework-engineered chimeras platform enables selectively targeted protein degradation. *Nat. Commun.* 2023, 14(1):4510.

[19] Zeng YC, Young OJ, Xiong Q, Si L, Ku MW, *et al.* DNA origami vaccine nanoparticles improve humoral and cellular immune responses to infectious diseases. *Nat. Biomed. Eng.* 2026, pp. 1–18.

[20] Ma N, Sun M, Shi H, Xue L, Zhang M, *et al.* A colorimetric/fluorescent dual-mode aptasensor for salmonella based on the magnetic separation of aptamers and a DNA-nanotriangle programmed multivalent aptamer. *Foods* 2023, 12(20):3853.

[21] Luo L, Li J, Zhou Y, Xiang D, Luan Y, *et al.* Spatially controlled DNA frameworks for sensitive detection and specific isolation of tumor cells. *Angew. Chem. Int. Ed.* 2024, 63(52):e202411382.

[22] Wamhoff EC, Banal JL, Bricker WP, Shepherd TR, Parsons MF, *et al.* Programming structured DNA assemblies to probe biophysical processes. *Annu. Rev. Biophys*. 2019, 48(1):395–419.

[23] Chen Y, Li F, Zhang S, Liu F, Mao C, *et al.* DNA framework-ensembled aptamers enhance fluid stability in circulating tumor cells capture for tumor treatment evaluation. *Angew. Chem.* 2025, 64(24):e202425252.

[24] Li M, Song L, Liu M, Guo R, Lin M, *et al.* Framework nucleic acid-programmed sensing interface with densely monodispersed probes. *ACS Nano* 2025, 19(25):23142–23150.
[25] Li M, Ding H, Lin M, Yin F, Song L, *et al.* DNA framework-programmed cell capture via topology-engineered receptor–ligand interactions. *J. Am. Chem. Soc.* 2019, 141(47):18910–18915.
[26] Szalai AM, Ferrari G, Richter L, Hartmann J, Kesici MZ, *et al.* Single-molecule dynamic structural biology with vertically arranged DNA on a fluorescence microscope. *Nat. Methods* 2025, 22(1):135–144.
[27] Krissanaprasit A, Key CM, Pontula S, LaBean TH. Self-assembling nucleic acid nanostructures functionalized with aptamers. *Chem. Rev.* 2021, 121(22):13797–13868.
[28] Liu Q, Ge Z, Mao X, Zhou G, Zuo X, *et al.* Valency-controlled framework nucleic acid signal amplifiers. *Angew. Chem. Int. Ed.* 2018, 57(24):7131–7135.
[29] Fu Y, Zeng D, Chao J, Jin Y, Zhang Z, *et al.* Single-step rapid assembly of DNA origami nanostructures for addressable nanoscale bioreactors. *J. Am. Chem. Soc.* 2013, 135(2):696–702.
[30] Sarwar A, Shakeel F, Fatima T, Amin R, Rizvi SNB, *et al.* DNA nanotechnology for next-generation biosensors: principles, strategies, and challenges. *Int. J. Biol. Macromol.* 2025, 329:147825.
[31] Lin C, Peng S, He J, Tang Y, Zou H, *et al.* An entropy-driven DNA timer fluorescence sensor for one-pot sequential detection of three respiratory viruses. *J. Mater. Chem. B* 2026, 14(20):6435–6444.
[32] Lin C, Liu Y, Yan H. Designer DNA nanoarchitectures. *Biochemistry* 2009, 48(8):1663–1674.
[33] Ke Y. Designer three-dimensional DNA architectures. *Curr. Opin. Struct. Biol.* 2014, 27:122–128.
[34] Saha R, Hayakawa D, Videbæk TE, Price M, Wei W, *et al.* Modular programming of interaction and geometric specificity enables assembly of complex DNA origami nanostructures. *Nat. Commun.* 2025, 16(1):11392.
[35] Fu TJ, Seeman NC. DNA double-crossover molecules. *Biochemistry* 1993, 32(13):3211–3220.
[36] Rothemund PWK. Folding DNA to create nanoscale shapes and patterns. *Nature* 2006, 440(7082):297–302.
[37] Wei B, Dai M, Yin P. Complex shapes self–assembled from single–stranded DNA tiles. *Nature* 2012, 485(7400):623–626.
[38] Yao G, Zhang F, Wang F, Peng T, Liu H, *et al.* Meta-DNA structures. *Nat. Chem.* 2020, 12(11):1067–1075.
[39] Seeman NC, Kallenbach NR. Design of immobile nucleic acid junctions. *Biophys. J.* 1983, 44(2):201–209.
[40] Winfree E, Liu F, Wenzler LA, Seeman NC. Design and self-assembly of two-dimensional DNA crystals. *Nature* 1998, 394(6693):539–544.
[41] LaBean TH, Yan H, Kopatsch J, Liu F, Winfree E, *et al.* Construction, analysis, ligation, and self-assembly of DNA triple crossover complexes. *J. Am. Chem. Soc.* 2000, 122(9):1848–1860.
[42] Yan H, Park SH, Finkelstein G, Reif JH, LaBean TH. DNA-templated self-assembly of protein arrays and highly conductive nanowires. *Science* 2003, 301 (5641):1882–1884.
[43] Zhang F, Nangreave J, Liu Y, Yan H. Structural DNA nanotechnology: state of the art and future perspective. *J. Am. Chem. Soc.* 2014, 136(32):11198–11211.
[44] He Y, Tian Y, Ribbe AE, Mao C. Highly connected two-dimensional crystals of DNA six-point-stars. *J. Am. Chem. Soc.* 2006, 128(50):15978–15979.

[45] Li F, Li J, Dong B, Wang F, Fan C, *et al.* DNA nanotechnology-empowered nanoscopic imaging of biomolecules. *Chem. Soc. Rev.* 2021, 50(9):5650–5667.
[46] Andersen ES, Dong M, Nielsen MM, Jahn K, Lind-Thomsen A, *et al.* DNA origami design of dolphin-shaped structures with flexible tails. *ACS Nano* 2008, 2(6):1213–1218.
[47] Qian L, Wang Y, Zhang Z, Zhao J, Pan D, *et al.* Analogic China map constructed by DNA. *Chin. Sci. Bull.* 2006, 51(24):2973–2976.
[48] Zhang F, Jiang S, Wu S, Li Y, Mao C, *et al.* Complex wireframe DNA origami nanostructures with multi-arm junction vertices. *Nat. Nanotechnol.* 2015, 10(9):779–784.
[49] Liu W, Zhong H, Wang R, Seeman NC. Crystalline two-dimensional DNA-origami arrays. *Angew. Chem. Int. Ed.* 2011, 50(1):264–267.
[50] Tikhomirov G, Petersen P, Qian L. Fractal assembly of micrometre-scale DNA origami arrays with arbitrary patterns. *Nature* 2017, 552(7683):67–71.
[51] Seeman NC. Nucleic acid junctions and lattices. *J. Theor. Biol.* 1982, 99(2):237–247.
[52] He Y, Ye T, Su M, Zhang C, Ribbe AE, *et al.* Hierarchical self-assembly of DNA into symmetric supramolecular polyhedra. *Nature* 2008, 452(7184):198–201.
[53] Chen J, Seeman NC. Synthesis from DNA of a molecule with the connectivity of a cube. *Nature* 1991, 350(6319):631–633.
[54] Goodman RP, Schaap IA, Tardin CF, Erben CM, Berry RM, *et al.* Rapid chiral assembly of rigid DNA building blocks for molecular nanofabrication. *Science* 2005, 310(5754):1661–1665.
[55] Zhang Y, Seeman NC. Construction of a DNA-truncated octahedron. *J. Am. Chem. Soc.* 1994, 116(5):1661–1669.
[56] Zhang C, Su M, He Y, Zhao X, Fang P, *et al.* Conformational flexibility facilitates self-assembly of complex DNA nanostructures. *Proc. Natl. Acad. Sci. U.S.A.* 2008, 105(31):10665–10669.
[57] Li Y, Tian C, Liu Z, Jiang W, Mao C. Structural transformation: assembly of an otherwise inaccessible DNA nanocage. *Angew. Chem. Int. Ed.* 2015, 54(20):5990–5993.
[58] Douglas SM, Dietz H, Liedl T, Hogberg B, Graf F, *et al.* Self-assembly of DNA into nanoscale three-dimensional shapes. *Nature* 2009, 459(7245):414–418.
[59] Dietz H, Douglas SM, Shih WM. Folding DNA into twisted and curved nanoscale shapes. *Science* 2009, 325(5941):725–730.
[60] Han D, Pal S, Nangreave J, Deng Z, Liu Y, *et al.* DNA origami with complex curvatures in three-dimensional space. *Science* 2011, 332(6027):342–346.
[61] Benson E, Mohammed A, Gardell J, Masich S, Czeizler E, *et al.* DNA rendering of polyhedral meshes at the nanoscale. *Nature* 2015, 523(7561):441–444.
[62] Iinuma R, Ke Y, Jungmann R, Schlichthaerle T, Woehrstein JB, *et al.* Polyhedra self-assembled from DNA tripods and characterized with 3D DNA-PAINT. *Science* 2014, 344(6179):65–69.
[63] Ong LL, Hanikel N, Yaghi OK, Grun C, Strauss MT, *et al.* Programmable self-assembly of three-dimensional nanostructures from 10^4 unique components. *Nature* 2017, 552(7683):72–77.
[64] Seeman NC. DNA in a material world. *Nature* 2003, 421(6921):427–431.
[65] Li J, Zhang Z, Liu R, Amini R, Salena BJ, *et al.* Discovery and translation of functional nucleic acids for clinically diagnosing infectious diseases: opportunities and challenges. *TrAC Trends Anal. Chem*. 2023, 158:116886.

[66] Zeng Y, Qi P, Wang Y, Chen C, Zhang D. DNA pom-pom nanostructure as a multifunctional platform for pathogenic bacteria determination and inactivation. *Biosens. Bioelectron.* 2021, 177:112982.

[67] Lv Z, Huang M, Li P, Xu M, Yao C, *et al.* Hybridization chain reaction-based DNA nanomaterials for biosensing, bioimaging and therapeutics. *Chin. Chem. Lett.* 2024, 35(2):108601.

[68] Feng Y, Liu Q, Zhao X, Chen M, Sun X, *et al.* Framework nucleic acid-based spatial-confinement amplifier for miRNA imaging in living cells. *Anal. Chem.* 2022, 94(6):2934–2941.

[69] Xu H, Zheng Y, Fang X, Cheng Y, Xu J, *et al.* Spatial confinement-based figure-of-eight nanoknots accelerated simultaneous detection and imaging of intracellular microRNAs. *Anal. Chim. Acta* 2023, 1250:340974.

[70] Guo T, Xiang Y, Lu H, Huang M, Liu F, *et al.* Interfacial DNA framework-enhanced background-to-signal transition for ultrasensitive and specific micro-RNA detection. *ACS Appl. Mater. Interfaces* 2022, 14(16):18209–18218.

[71] Qiu H, Yang Q, Qiu H, Hu Z, Kong F, *et al.* Single-nucleotide level base recognition through a complex DNA tetrahedron probe. *Microchem. J.* 2025, 212:113485.

[72] Li D, Liu L, Huang Q, Tong T, Zhou Y, *et al.* Recent advances on aptamer-based biosensors for detection of pathogenic bacteria. *World J. Microbiol. Biotechnol.* 2021, 37(3):45.

[73] Stangherlin S, Lui N, Lee JH, Liu J. Aptamer-based biosensors: from SELEX to biomedical diagnostics. *TrAC Trends Anal. Chem*. 2025, 191:118349.

[74] da Rosa G, de Castro M, García Velásquez VM, Pintos S, Benedetto J, *et al.* Aptamers meet structural bioinformatics, computational chemistry, and artificial intelligence. *Wires Comput. Mol. Sci.* 2025, 15(5):e70050.

[75] Fu K, Zheng J, Zhang Y, Liu C, Zhang W, *et al.* Construction of a multiplex biosensor for the on-site rapid detection of phthalates in biological fluids based on single-stranded DNA aptamers. *J. Hazard. Mater.* 2025, 499:140164.

[76] Zhu F, Yu H, Zhao Q. CRISPR/Cas12a-amplified aptamer switch microplate assay for small molecules. *Anal. Chem.* 2024, 96(17):6853–6859.

[77] Wang S, Elmorsy A, Tüzün D, Schmidt L, Freko S, *et al.* Dual-channel interdigitated aptamer-based sensors for rapid small-molecule detection in biofluids. *Angew. Chem. Int. Ed.* 2026, 65(27):e8361141.

[78] Ahmadi Y, Umrekar TR, Mutter N, Beeby M, Barišić I. DNA origami-enhanced binding of aptamers to staphylococcus aureus cells. *Biosens. Bioelectron.: X* 2024, 16:100436.

[79] Tu T, Huan S, Feng X, Ke G, Li L, *et al.* Spatial confinement of a dual activatable DNAzyme sensor in the cavity of a DNA nanocage for logic-gated molecular imaging. *Angew. Chem. Int. Ed.* 2025, 64(15):e202424684.

[80] Frohnmeyer E, Tuschel N, Sitz T, Hermann C, Dahl GT, *et al.* Aptamer lateral flow assays for rapid and sensitive detection of cholera toxin. *Analyst* 2019, 144(5):1840–1849.

[81] Wang G, Zhang Y, Tang S, Chen S, Zou F, *et al.* Multivalent aptamer nanoscaffold cytosensor for glioma circulating tumor cells during epithelial–mesenchymal transition. *Biosens. Bioelectron.* 2023, 226:115140.

[82] Xu J, Zhang X, Yan C, Qin P, Yao L, *et al.* Trigging isothermal circular amplification-based tuning of rigorous fluorescence quenching into complete restoration on a multivalent aptamer probe enables ultrasensitive detection of salmonella. *Anal. Chem.* 2022, 94(2):1357–1364.

[83] Salim IN, Reay R, Denby C, Halloran C, Ngo TA, *et al.* DNA origami and their application in biosensors. *Biosensors* 2026, 16(5):247.

[84] Zhang P, Liu X, Liu P, Wang F, Ariyama H, *et al.* Capturing transient antibody conformations with DNA origami epitopes. *Nat Commun*. 2020, 11:3114.

[85] Pradhan S, Swanson CJ, Leff C, Tengganu I, Bergeman MH, *et al.* Viral attachment blocking chimera composed of DNA origami and nanobody inhibits pseudorabies virus infection *in vitro*. *ACS Nano* 2023, 17(23):23317–23330.

[86] Rosier BJ, Cremers GA, Engelen W, Merkx M, Brunsveld L, *et al.* Incorporation of native antibodies and fc-fusion proteins on DNA nanostructures via a modular conjugation strategy. *Chem Commun*. 2017, 53(53):7393–7396.

[87] Ouyang X, De Stefano M, Krissanaprasit A, Bank Kodal AL, Bech Rosen C, *et al.* Docking of antibodies into the cavities of DNA origami structures. *Angew. Chem. Int. Ed.* 2017, 56(46):14423–14427.

[88] Norden DM, Navia CT, Sullivan JT, Doranz BJ. The emergence of cell-based protein arrays to test for polyspecific off-target binding of antibody therapeutics. *MAbs* 2024, 16(1):2393785.

[89] Bauer M, Strom M, Hammond DS, Shigdar S. Anything you can do, I can do better: can aptamers replace antibodies in clinical diagnostic applications? *Molecules* 2019, 24(23):4377.

[90] Resina L, Alemán C, Ferreira FC, Esteves T. Protein-imprinted polymers: how far have “plastic antibodies” come? *Biotechnol. Adv.* 2023, 68:108220.

[91] Yin F, Zhang S, Chen H, Li Q, Zuo X, *et al.* DNA framework nanoruler-directed surface fluorescence enhancement as a sensing platform for MicroRNA detection. *J. Am. Chem. Soc.* 2025, 147(31):28484–28491.

[92] Zhang R, Zuo X, Yin F. Nucleic acid framework-enabled spatial organization for biological applications. *Chem. Bio Eng*. 2024, 2(2):71–86.

[93] Wang W, Wang W, Chen Y, Lin M, Chen Y, *et al.* Superlarge, rigidified DNA tetrahedron with a Y-shaped backbone for organizing biomolecules spatially and maintaining their full bioactivity. *ACS Nano* 2024, 18(28):18257–18281.

[94] Lee DG, Kim YY, Yang H, Song YK. Engineering versatile supramolecular structures with tetravalent DNA-traptavidin building blocks. *Nanoscale Adv*. 2025, 7(20):6417–6421.

[95] Zhou X, Zhao M, Duan X, Guo B, Cheng W, *et al.* Collapse of DNA tetrahedron nanostructure for “off–on” fluorescence detection of DNA methyltransferase activity. *ACS Appl. Mater. Interfaces* 2017, 9(46):40087–40093.

[96] Brannetti S, Gentile S, Chamorro-Garcia A, Barbero L, Del Grosso E, *et al.* Decorated DNA-based scaffolds as lateral flow biosensors. *Angew. Chem. Int. Ed. Engl.* 2023, 62(47):e202313243.

[97] Grzedowski AJ, Jun D, Mahey A, Zhou GC, Fernandez R, *et al.* Engineering DNA nanocube SAM scaffolds for FRET-based biosensing: interfacial characterization and sensor demonstration. *J. Am. Chem. Soc.* 2024, 146(46):31560–31573.

[98] Zhang B, Tian T, Xiao D, Gao S, Cai X, *et al.* Facilitating in situ tumor imaging with a tetrahedral DNA framework-enhanced hybridization chain reaction probe. *Adv. Funct. Mater.* 2022, 32(16):2109728.

[99] Zhao M, Zhang J, Wang L, Lu N. Tetrahedral DNA framework-engineered magnetic nanozyme for visual biomarker sensing via alkaline phosphatase-triggered signal switching. *Anal. Chem.* 2025, 97(36):19505–19516.
[100] Zhu D, Wei Y, Sun T, Zhang C, Ang L, *et al.* Encoding DNA frameworks for amplified multiplexed imaging of intracellular microRNAs. *Anal. Chem.* 2021, 93(4):2226–2234.
[101] Yin F, Zhao H, Lu S, Shen J, Li M, *et al.* DNA-framework-based multidimensional molecular classifiers for cancer diagnosis. *Nat. Nanotechnol.* 2023, 18(6):677–686.
[102] Ge Z, Fu J, Liu M, Jiang S, Andreoni A, *et al.* Constructing submonolayer DNA origami scaffold on gold electrode for wiring of redox enzymatic cascade pathways. *ACS Appl. Mater. Interfaces* 2019, 11(15):13881–13887.
[103] Jeon B, Guareschi MM, Stewart JM, Wu E, Gopinath A, *et al.* Modular DNA origami–based electrochemical detection of DNA and proteins. *Proc. Natl. Acad. Sci. U.S.A.* 2025, 122(1):e2311279121.
[104] Tsang E, Lund LM, Birkedal V, Gothelf KV. Single-molecule nucleic acid detection with a reconfigurable rotating DNA origami nanodevice. *ACS Nano* 2026, 20(5):4607–4616.
[105] Yamanaka K, Vestergaard MC, Tamiya E. Printable electrochemical biosensors: a focus on screen-printed electrodes and their application. *Sensors* 2016, 16(10):1761.
[106] Hou Y, Wang J, Jiang Y, Lv C, Xia L, *et al.* A colorimetric and electrochemical immunosensor for point-of-care detection of enterovirus 71. *Biosens. Bioelectron.* 2018, 99:186–192.
[107] Su J, Ke Y, Maboyi N, Zhi X, Yan S, *et al.* CRISPR/Cas12a powered DNA framework-supported electrochemical biosensing platform for ultrasensitive nucleic acid analysis. *Small Methods* 2021, 5(12):2100935.
[108] Li F, Li J, Yang W, Yang S, Chen C, *et al.* Framework-hotspot enhanced trans cleavage of CRISPR-Cas12a for clinical samples detection. *Angew. Chem. Int. Ed.* 2023, 62(32):e202305536.
[109] Hao J, Gong X, Duan X, Qin W, Ren H, *et al.* Ultrasensitive electrochemical detection of parvovirus B19 DNA by combining CRISPR-Cas12a and multivalent framework nucleic acids. *Anal. Methods* 2025, 17(46):9357–9364.
[110] Majikes JM, Cho S, Cleveland TE, Liddle JA, Balijepalli A. Variable gain DNA nanostructure charge amplifiers for biosensing. *Nanoscale* 2024, 16(45):20893–20902.
[111] Chen G, Liu X, Liu X, Wang J, Cheng H, *et al.* Programmable DNA framework-based logic-gated dual-distance regulation for photoelectrochemical multiplex and sensitive detection of waterborne viruses. *Anal. Chem.* 2026, 98(8):6350–6362.
[112] Soleja N, Mohsin M. Exploring the landscape of FRET-based molecular sensors: design strategies and recent advances in emerging applications. *Biotechnol. Adv.* 2024, 77:108466.
[113] Chauhan N, Xiong Y, Ren S, Dwivedy A, Magazine N, *et al.* Net-shaped DNA nanostructures designed for rapid/sensitive detection and potential inhibition of SARS-CoV-2 virus. *J. Am. Chem. Soc.* 2023, 145(37):20214–20228.
[114] Zhou L, Xiong Y, Dwivedy A, Zheng M, Cooper L, *et al.* Bioinspired designer DNA NanoGripper for virus sensing and potential inhibition. *Sci. Robot*. 2024, 9(96):eadi2084.
[115] Li Y, Huo H, Han S, Deng C, Liu W, *et al.* A highly antifouling and dual-responsive PEC-FL biosensor for prostate-specific antigen based on DNA micelle signal converter and 3-D self-supporting multivariate heterojunction. *IEEE Sens. J.* 2025, 25(6):9282–9289.

[116] Wei L, Wang Z, Dong Y, Yu D, Chen Y. Enhanced CRISPR/Cas12a fluorimetry via a DNAzyme-embedded framework nucleic acid substrate. *Anal. Chem.* 2024, 96(41):16453–16461.
[117] Zhang X, Peng Y, Yao L, Shang H, Zheng Z, *et al.* Self-assembly of multivalent aptamer-tethered DNA monolayers dedicated to a fluorescence polarization-responsive circular isothermal strand displacement amplification for *salmonella* assay. *Anal. Chem.* 2023, 95(4):2570–2578.
[118] Huang Q, Chen B, Shen J, Liu L, Li J, *et al.* Encoding fluorescence anisotropic barcodes with DNA frameworks. *J. Am. Chem. Soc.* 2021, 143(28):10735–10742.
[119] Xie J, Xie T, Luo Y, Mao K, Huang C, *et al.* Octopus-like DNA nanostructure coupled with graphene oxide enhanced fluorescence anisotropy for hepatitis B virus DNA detection. *Chin. Chem. Lett.* 2024, 35(6):109137.
[120] Lim J, Koprowski K, Stavins R, Xuan N, Hoang TH, *et al.* Point-of-care multiplex detection of respiratory viruses. *ACS Sens.* 2024, 9(8):4058–4068.
[121] Jian D, Wang B, Huang H, Meng X, Liu C, *et al.* Sunlight based handheld smartphone spectrometer. *Biosens. Bioelectron.* 2019, 143:111632.
[122] Xiao W, Sun C, Chen S, Xue L, Wei H, *et al.* Smartphone-based fluorescence/colorimetric dual-mode aptasensor for the detection of *salmonella* using multivalent aptamer and CHA amplification. *ACS Sens.* 2025, 10(9):6542–6552.
[123] Chen H, Huang L, Luo X, Shi H, Song Y, *et al.* Programmable DNA nanostructure-based self-powered biosensor for point-of-care opportunistic pathogens detection. *Sens. Actuators B Chem.* 2026, 448:139063.
[124] Du T, Ding F, Ma X, Luo Y, Zhu D, *et al.* Ultrasensitive detection of monkeypox virus: harnessing synergistic CRISPR-driven signal amplification on a DNA tetrahedron-mediated sensing interface. *Biosens. Bioelectron.* 2026, 298:118441.
[125] Yaadav R, Trofymchuk K, Dass M, Behrendt V, Hauer B, *et al.* Bringing attomolar detection to the point-of-care with nanopatterned DNA origami nanoantennas. *Adv Mater.* 2025, 37(40):e07407.
[126] Dou Y, Su J, Chen S, Li T, Wang L, *et al.* A smartphone-based three-in-one biosensor for co-detection of SARS-CoV-2 viral RNA, antigen and antibody. *Chem. Commun.* 2022, 58(41):6108–6111.
[127] Pin X, Cui J, Zhi C, Shiu SCC, Cui J, *et al.* Nanoplasmonic optical fiber sensing of SARS-CoV-2 nucleocapsid protein using an aptamer-DNA tetrahedron interface. *J. Nanobiotechnol.* 2026, 24(1):393.
[128] Kwon PS, Ren S, Kwon SJ, Kizer ME, Kuo L, *et al.* Designer DNA architecture offers precise and multivalent spatial pattern-recognition for viral sensing and inhibition. *Nat. Chem*. 2020, 12(1):26–35.
[129] Zhang C, Guo X, Zheng J, Feng Y, Wu W, *et al.* DNA-directed electrochemiluminescence nanosphere with electrocatalysis-enhanced microfluidic arrays for rapid multibacterial detection. *Sci. Adv*. 2025, 11(50):eady3070.
[130] Wang M, Li L, Wei L, Han Y, Chen Y. Multiplexed pathogenic bacteria detection via a two-dimensional encoded fluorescent microsphere system. *Nano Lett.* 2025, 25(6):2256–2265.
[131] Enebral-Romero E, García-Fernández D, Gutiérrez-Gálvez L, López-Diego D, Luna M, *et al.* Bismuthene—tetrahedral DNA nanobioconjugate for virus detection. *Biosens. Bioelectron.* 2024, 261:116500.

[132] Wu Y, Ji D, Dai C, Kong D, Chen Y, *et al.* Triple-probe DNA framework-based transistor for SARS-CoV-2 10-in-1 pooled testing. *Nano Lett.* 2022, 22(8):3307–3316.
[133] Min Z, Xie J, Xiao M, Li J, Peng X, *et al.* A DNA triangular prism-based multitargeting transistor for ultrasensitive detection of respiratory virus. *Anal. Chem.* 2025, 97(38):20850–20858.
[134] Zhan X, Zhou J, Jiang Y, An P, Luo B, *et al.* DNA tetrahedron-based CRISPR bioassay for treble-self-amplified and multiplex HPV-DNA detection with elemental tagging. *Biosens. Bioelectron.* 2023, 229:115229.
[135] Patnaik A, Kayal T, Basu S. Polymicrobial infections: a comprehensive review on current context, diagnostic bottlenecks and future directions. *Acta Microbiol. Hell.* 2025, 70(4):39.
[136] Tang L, Yang J, Liu Z, Mi Q, Niu L, *et al.* Design nanoprobe based on DNA tetrahedron supported hybridization chain reaction and its application to *in situ* analysis of bacteria. *Chem. Eng. J.* 2023, 466:143099.
[137] Wang H, Chen R, He Y, Zhu X, Yu Z, *et al.* Controllable self-cleaning FET self-assembled RNA-cleaving DNAzyme based DNA nanotree for culture-free Staphylococcus aureus detection. *J. Nanobiotechnol*. 2024, 22(1):414.
[138] Tang L, Niu L, Wang P, Cheng L, Zhang R, *et al.* Tetrahedron supported click ligation initiated by dual recognition for precise bacterial analysis. *Biosens. Bioelectron*. 2022, 210:114342.
[139] Xi C, Zhang J, Song L, Zhang Y, Wang S, *et al.* DNA framework-encoded digital recorder for bacterial discrimination. *ACS Nano* 2026, 20(9):8045–8054.
[140] Liu L, Feng X, Zou Y, Xia T, Kong F, *et al.* Anti-interference detection of antibiotic resistance genes via tetrahedral DNA framework–velcro capturing py-HOF@Ti3C2 MXene. *J. Hazard. Mater.* 2025, 492:138146.
[141] Wang X, Shen X, Li J, Ge X, Ouyang J, *et al.* Biomineralization of DNA nanoframeworks for intracellular delivery, on-demand diagnosis, and synergistic cancer treatments. *Anal. Chem.* 2022, 94(48):16803–16812.
[142] Li B, Liu Y, Wang H, Huang X, Li W, *et al.* High-precision DNA nanostructure-templated silicification via modified silanes. *J. Am. Chem. Soc.* 2025, 147(49):44995–45003.
[143] Jing X, Wang H, Huang J, Liu Y, Li Z, *et al.* Molecular tuning of DNA framework–programmed silicification by cationic silica cluster attachment. *Proc. Natl. Acad. Sci. U.S.A.* 2026, 123(6):e2529275123.
[144] Ober MF, Baptist A, Wassermann L, Heuer-Jungemann A, Nickel B. *In situ* small-angle X-ray scattering reveals strong condensation of DNA origami during silicification. *Nat Commun*. 2022, 13(1):5668.
[145] Zhao H, Yi D, Li L, Zhao Y, Li M. Modular weaving DNAzyme in skeleton of DNA nanocages for photoactivatable catalytic activity regulation. *Angew. Chem.* 2024, 136(18):e202404064.
[146] Brown TM, Fakih HH, Saliba D, Asohan J, Sleiman HF. Stabilization of functional DNA structures with mild photochemical methods. *J. Am. Chem. Soc.* 2023, 145(4):2142–2151.
[147] Bai T, Zhang J, Huang K, Wang W, Chen B, *et al.* Reconfiguration of DNA nanostructures induced by enzymatic ligation treatment. *Nucleic Acids Res.* 2022, 50(14):8392–8398.
[148] Liu X, Jing X, Liu P, Pan M, Liu Z, *et al.* DNA framework-encoded mineralization of calcium phosphate. *Chem* 2020, 6(2):472–485.

[149] Wang C, Wang W, Xu Y, Zhao X, Li S, *et al.* Tetrahedral DNA framework-programmed electrochemical biosenors with gold nanoparticles for ultrasensitive cell-free DNA detection. *Nanomaterials* 2022, 12(4):666.

[150] Chu J, Ejaz A, Lin KM, Joseph MR, Coraor AE, *et al.* Single-molecule fluorescence multiplexing by multi-parameter spectroscopic detection of nanostructured FRET labels. *Nat. Nanotechnol*. 2024, 19(8):1150–1157.

[151] Kim J, Kwon JH, Jang J, Lee H, Kim S, *et al*. Rapid and background-free detection of avian influenza virus in opaque sample using NIR-to-NIR upconversion nanoparticle-based lateral flow immunoassay platform. *Biosens. Bioelectron.* 2018, 112:209–215.

[152] Reichmuth DS, Wang SK, Barrett LM, Throckmorton DJ, Einfeld W, *et al.* Rapid microchip-based electrophoretic immunoassays for the detection of swine influenza virus. *Lab Chip* 2008, 8(8):1319–1324.